A Y-linked duplication of anti-Mullerian hormone is the sex determination gene in threespine stickleback

Matthew J Treaster[1], Jenny McCann[1], Kyra S Solovei[1], Ryan J Palmieri[1], Michael A White[1*]

[1] Department of Genetics, University of Georgia, Athens, Georgia

* Corresponding Author

Email: Whitem@uga.edu

Abstract

Many taxa have independently evolved genetic sex determination where a single gene located on a sex chromosome controls gonadal differentiation. The gene anti-Mullerian hormone (*amh*) has convergently evolved as a sex determination gene in numerous vertebrate species, but how this gene has repeatedly evolved this novel function is not well understood. In the threespine stickleback (*Gasterosteus aculeatus*), *amh* was duplicated onto the Y chromosome (*amhy*) ~22 million years ago. To determine whether *amhy* is the primary sex determination gene, we used CRISPR/Cas9 and transgenesis to show that *amhy* is necessary and sufficient for male sex determination, consistent with the function of a primary sex determination gene. We find that *amhy* contributes to a higher total dosage of *amh* early in development and likely contributes to differential germ cell proliferation key to sex determination. The creation of sex reversed lines also allowed us to investigate the genetic basis of secondary sex characteristics. Threespine stickleback have striking differences in behavior and morphology between sexes. Here we show one of the classic traits important for reproductive success, blue male nuptial coloration, is controlled by both sex-linked genetic factors as well as hormonal factors independent of sex chromosome genotype. This research establishes stickleback as a model to investigate how *amh* regulates gonadal development and how this gene repeatedly evolves novel function in sex determination. Analogous to the “four core genotypes” model in house mice, sex-reversed threespine stickleback offer a new vertebrate model for investigating the separate contributions of gonadal sex and sex chromosomes to sexual dimorphism.

Author Summary

Many species have evolved sex chromosomes like the XY system found in humans and other mammals. While sex chromosomes can contain hundreds of genes, a single sex determination gene found on the sex chromosomes controls whether the gonad develops into

an ovary or testis. Many different sex determination genes have been identified across species, but we still have much to learn about how different sex determination genes control the same process of sex determination. Here, we show that an extra copy of the gene anti-Mullerian hormone on the Y chromosome of threespine stickleback fish is the sex determination gene responsible for initiating testis development. By manipulating this sex determination gene, we are now able to generate male and female stickleback with either XX or XY sex chromosome genotypes. This allows us to investigate the role of sex chromosomes in fitness and development outside of sex determination which is not possible in many models. Surprisingly, we find that the Y chromosome is not necessary for male fertility in stickleback. We also show that a key secondary sex characteristic, male mating color, is controlled both by hormones produced by the gonad as well as independent genetic factors on the sex chromosomes.

Introduction

For species that have two discrete sexes, sex determination is the process that designates whether an individual will become male or female [1,2]. While this process is essential to the fitness and survival of a species, it is regulated by a surprising variety of initial cues and can incorporate a range of extrinsic signals as well as intrinsic genetic factors often located on sex chromosomes [1–3]. Numerous eukaryotic taxa have convergently evolved sex chromosomes, such as the XX-XY system found in mammals, to regulate this critical developmental process [1,2]. Sex chromosomes are derived from a pair of autosomes after one of these autosomes acquires a sex determining (SD) gene [4]. Suppression of recombination around this gene leads to sequence divergence of the two autosomes into a pair of divergent sex chromosomes [4]. Why this recombination suppression occurs is not clear; however, the prevailing model is that suppressed recombination will be selected for to link an SD gene with nearby sexually antagonistic mutations that are beneficial to one sex but detrimental to the other

61 [4–6]. Empirically testing which genes on sex chromosomes are sexually antagonistic remains
62 challenging, as these genes are perfectly linked to the sex determination gene. Thus, evaluating
63 the fitness effects of sex-limited loci in the opposite sex (i.e. Y-linked loci in females) is not
64 possible in most systems. Novel systems where sex can be isolated from other loci on the sex
65 chromosome would be helpful for testing these theoretical models of sex chromosome
66 evolution.

67 A wide variety of genes have evolved novel function as SD genes, but some genes
68 appear predisposed to acquiring this role and have convergently evolved as SD genes in
69 distantly related taxa [7]. *Sox3*, the ancestor of the mammalian SD gene, *Sry,* also acts as the
70 SD gene in the Indian rice fish (*Oryzias dancena*) [8]. SD genes derived from *dmrt1* are found in
71 birds [9], the African clawed frog (*Xenopus laevis*) [10], and medaka (*Oryzias latipes*) [11,12].
72 The most prevalent SD gene among vertebrates by far is *anti-Mullerian hormone* (*amh*) [7].
73 Independently acquired Y-linked copies of *amh* or its dedicated receptor, *amhrII*, have been
74 identified in at least twelve different clades of teleost fish [13–24] as well as in monotremes [25].
75 These Y-linked copies of *amh* and *amhrII* are presumed to be SD genes in all of these taxa.
76 Although *amh* accounts for over one quarter of identified SD genes in vertebrates, how *amh*
77 controls this critical developmental process and evolves novel function in sex determination is
78 not clear [7].

79 *Amh* is a member of the transforming growth factor beta (TGF-β) family of proteins that
80 are shared across vertebrates (Reviewed in [26,27]). *Amh* is unique among TGF-β hormones as
81 it has only one identified type II receptor, *amhrII*, of which *amh* is the only known ligand [28–30].
82 *Amh* and its receptor were first identified for their role in reproductive tract development in
83 mammals, where secretion of Amh by the developing testes causes regression of the primordial
84 female reproductive tract, the Müllerian ducts [31]. Disruption of *amh* signaling in teleosts, which
85 lack Müllerian ducts, causes over proliferation of germ cells in the gonad and can interfere with
86 sex determination, even in species were *amh* is not the SD gene [32–34]. This suggests the

87 ancestral function of *amh* is likely in germ cell proliferation and maintenance which, if altered,
88 can disrupt sex determination, but how this disruption occurs is not clear. It also is not known
89 whether Y-linked copies of *amh* that have convergently evolved function in sex determination
90 control the downstream differentiation network in the same way or if *amh* can regulate sex
91 differentiation through a variety of distinct mechanisms.

92 Species of stickleback fish (family Gasterosteidae) have multiple, independently evolved
93 sex chromosome systems, making them an ideal model for investigating the origins of sex
94 chromosomes and SD genes [20,35–38]. Two separate duplications of *amh* that are associated
95 with male sex have been identified within stickleback fish. In the genus *Gasterosteus*, *amh* was
96 duplicated from autosome 8 onto autosome 19 approximately 22 million years ago (mya),
97 leading to the evolution of a Y chromosome [20,39]. An independent duplication of *amh* onto
98 chromosome 20 was identified in the brook stickleback, *Culea inconstans*. This duplication
99 differs from the ancestral copy on autosome 8 by only a handful of single nucleotide
100 polymorphisms (SNPs), suggesting this duplication occurred much more recently than in the
101 genus *Gasterosteus* [22,40]. Consistent with its recent acquisition, the duplicate copy of *amh* is
102 not a fully penetrant SD gene, and its association with male sex varies across populations [40].
103 This provides a unique opportunity to examine the convergence evolution of *amh* as an SD
104 gene at two dramatically different stages of sex chromosome evolution.

105 The threespine stickleback (*Gasterosteus aculeatus*) is a powerful emerging model for
106 evolutionary and developmental biology with a robust set of genomic and functional genetic
107 tools [41,42]. Their small size, large clutch sizes, and relatively short generation time make them
108 a highly tractable model for studying the developmental mechanisms of *amh* as an SD gene.
109 Threespine stickleback also have many well-studied sexually dimorphic traits and mating
110 behaviors that have provided substantial insight into the evolution of sexual dimorphism and its
111 effect on fitness [43–64]. Like other members of its genus, threespine stickleback have retained
112 a functional copy of autosomal *amh* on chromosome 8 as well as the Y-linked *amhy*. The AMH

113 prodomain and TGF-β signaling domain within *amhy* are conserved (S1 Fig), indicating the Y-
114 linked duplicate is likely functional [20]. In addition, *amhy* is expressed in larvae around the time
115 of sex determination, consistent with a role in initiating male development [20]. Beyond this, it is
116 unknown whether *amhy* has a functional role in male sex determination. In this study, we show
117 that *amhy* is both necessary and sufficient for male sex determination in the threespine
118 stickleback, demonstrating that it is the SD gene in this species. We also perform RNA-seq of
119 stickleback embryos and larvae to characterize expression of *amhy* and early transcriptional
120 differentiation of males and females. Our findings establish stickleback fish as a premier model
121 to study both the molecular mechanisms of *amh* based sex determination as well as the
122 convergent evolution of *amh* as a SD gene in vertebrates.
123

124 # Results

125 **CRISPR/Cas9 knockout of amhy caused male-to-female sex reversal in XY fish.**

126 If *amhy* is the SD gene in threespine stickleback, it should be both necessary and
127 sufficient for male sex determination. To test this, we first knocked out function of *amhy* in XY
128 fish using CRISPR/Cas9. We designed two sgRNAs targeting exon 1 and exon 3 of *amhy* (Fig
129 1). We injected stickleback embryos from lab-reared fish derived from two independent marine
130 populations (Port Gardner Bay and Japan Pacific Ocean) with CRISPR ribonucleoprotein (RNP)
131 made with one of the two sgRNAs. 8/17 (47%) of F0 XY fish injected with RNP exhibited male-
132 to-female sex reversal. For all eight XY sex reversed fish, we observed ovaries with all cell
133 types seen in wildtype ovaries (S2A Fig).

134 F0 crispants are often mosaic for mutations induced by CRISPR/Cas9 gene editing (S2B
135 Fig), which can cause variation in observed phenotypes. To generate non-mosaic F1 gene-
136 edited fish, we used two F0 XY males that had heritable germline mutations in *amhy* but were
137 not sex reversed, indicating they likely did not have *amhy* mutations in cell-lineages important

138 for sex determination. Sperm from these fish were used to fertilize eggs from wildtype XX
139 females. F1 offspring from these crosses inherited frameshift mutations in *amhy*, identified by
140 Sanger sequencing (S3 Fig). We analyzed five F1 males from one F0 crispant with mutations in
141 exon 1 and 21 F1 males from one F0 crispant with mutations in exon 3. All 26 F1 fish exhibited
142 complete male-to-female sex reversal and developed ovaries morphologically and histologically
143 indistinguishable from wildtype XX females (Fig 1C). No F1 XY fish showed development of
144 testis or ambiguous gonad tissue with any visible spermatocyte production. We identified three
145 loss of function alleles in exon 1 of *amhy* (Fig 1A) and one in exon 3 (Fig 1B). In ten F1 fish, the
146 region of *amhy* in exon 3 targeted by CRISPR/Cas9 could not be amplified. PCR of exons 1 and
147 7 showed the presence of these distal portions of *amhy*, but PCR primers spanning a large
148 putative deletion all failed to amplify, suggesting a chromosomal rearrangement disrupted *amhy*
149 in these fish. As a specific mutation could not be positively identified, these samples were
150 excluded from further analysis and final counts.

151 We analyzed the expression of canonical male differentiation genes *amh* and *dmrt1* and
152 female differentiation genes *foxl2* and *cyp19a1a* using *in situ* hybridization on wildtype and F1
153 XY *amhy*-KO ovaries (Fig 2, S4 Fig). We also analyzed *gsdf* as a positive control, as this gene
154 is expected to be expressed in somatic gonadal cells of both sexes [65]. Both wildtype and sex
155 reversed ovaries showed expression of *foxl2* and *cyp19a1a* in somatic cells. Expression of *amh*
156 and *dmrt1* was minimal and restricted to oocytes when present as has been observed in some
157 species of fish [21,66–69]

158 Knockout of *amh* or *amhrII* in teleost species without amh-based sex determination has
159 caused male-to-female sex reversal, including in lab strains of zebrafish which lack sex
160 chromosomes (reviewed in [70]) and medaka which have an XX-XY system with a *dmrt1*
161 derived SD gene [32]. Thus, it is possible that off-target mutations of the paralogous *amh* could
162 contribute to the sex reversal observed in F1 *amhy* mutants. Both sgRNAs have multiple
163 mismatches to their homologous region in *amh*, and we verified that all F1 XY *amhy*-KO

164 females did not have mutations within *amh* by sanger sequencing (S5 Fig). This demonstrates
165 that the sex reversal phenotype was not caused by mutations of *amh*. We also investigated
166 whether the sex reversal phenotype was caused by a mutation at an unknown autosomal locus.
167 Such an autosomal mutation must be dominant since we observed male-to-female sex reversal
168 in heterozygous XY F1 fish. F1 XX siblings of sex reversed XY fish would also be heterozygous
169 for this mutation, and half of their F2 XY progeny would be sex reversed. We crossed two F1 XX
170 females with wildtype XY males and phenotyped F2 offspring for sex reversal. All 16 F2 XY fish
171 were phenotypically male, indicating that sex reversal in F1 XY *amhy*-KO fish was not caused
172 by an off-target autosomal mutation.
173

174 **Introduction of an *amhy* transgene caused female-to-male sex reversal in XX fish.**

175 To determine if *amhy* is sufficient for male sex determination, we created a construct
176 (pT2-5amhy2.5,Xla.Ef1a:EGFP) containing an 11 kb region of the Y chromosome which
177 includes *amhy*, 5 kb of upstream sequence, and 2.5 kb of downstream sequence (S6 Fig). By
178 including the surrounding non-coding sequences, we aimed to recapitulate the endogenous
179 expression patterns of *amhy.* An Xla.Ef1a:EGFP cassette downstream of *amhy* was included to
180 facilitate the screening of injected embryos for transgene integration (Fig 3C). These
181 components were flanked by *Tol2* transposon sequences to facilitate random integration into the
182 genome by the Tol2 transposase [71,72]. 16 F0 XX fish showed positive GFP expression and
183 successful transgene integration, detected through PCR genotyping (Fig 3D). At reproductive
184 age, all 16 F0 XX *Tg(amhy,EGFP)* were female-to-male sex reversed, developing testes rather
185 than ovaries (Fig 3A). All 10 control F0 XX fish injected with the control Xla.ef1a:EGFP
186 transgene showed positive presence of the transgene but did not show any signs of sex
187 reversal and developed cytologically normal ovaries (Fig 3B). We also analyzed the expression
188 of *amh, dmrt1, foxl2*, *cyp19a1a,* and *gsdf* using *in situ* hybridization on wildtype and F0 XX
189 *Tg(amhy,EGFP)* testes (Fig 2, S7 Fig). Both wildtype and sex reversed testes showed strong

190 expression of *amh* and *dmrt1* in somatic cells and no discernable expression of *foxl2* or
191 *cyp19a1a*.
192 We attempted to constitutively express *amhy* using a synthetic exon-only coding
193 sequence with an N-terminus FLAG tag joined to a 3' EGFP by a P2A self-cleaving peptide
194 [73,74]. Plasmids were made using the *D. rerio* ubiquitin promoter [75] or the *X. laevis* ef1a
195 promoter [76] to drive expression of the amhy,EGFP construct (S6 Fig). Transgenes with the
196 respective promoter driving expression of only EGFP were used as controls. Somatic EGFP
197 expression was observed with both control transgenes indicating these commonly used
198 vertebrate constitutive promoters can drive expression in stickleback. Neither the
199 Dre.Ubi:amhy,EGFP nor the Xla.Ef1a:amhy,EGFP transgene produced any larvae with visible
200 EGFP expression, indicating that the *amhy* transgenes were failing to integrate or be actively
201 expressed in any embryos. *Amh* has been overexpressed successfully in mouse [77], chicken
202 [78], and Nile tilapia [16], and the P2A peptide has been successfully used in stickleback
203 overexpression constructs [79], indicating that overexpression alone or the presence of a P2A
204 peptide was likely not responsible for the failure of this construct. One possibility is introns of
205 *amhy* may contain essential functional elements needed for gene expression of *amhy* in
206 threespine stickleback. The presence of introns has been shown to impact gene expression,
207 even under the regulation of non-native constitutive promoters [80,81].
208

209 **Sex reversed *amhy* mutants produce viable gametes but are subfertile.**

210 Female-to-male sex reversed F0 XX fish had varied fertility. Four of the 16 XX
211 *Tg(amhy,EGFP)* males had testes morphologically resembling those of a fertile, wildtype male.
212 12 XX males had abnormally small and underdeveloped testes. We performed crosses with all
213 four males with mature testes with wildtype XX females. We identified viable, successfully
214 fertilized embryos by the presence of a gastrula and active epiboly 12 to 24 hours post
215 fertilization (hpf). One male was extremely subfertile and only 3% of embryos were viable

216 (n=911). The remaining three males showed normal viability rates (80% n=97; 94% n=89, 98%
217 n=235), similar to viability rates of three wildtype males (73% n=314, 87% n=252, 97% n=291)
218 (S1 Table). One fertile male also produced offspring with somatic GFP expression at a very low
219 frequency (7%, n=231), indicating a heritable germline integration of the transgene containing
220 the constitutive Ef1a:EGFP cassette had occurred. Histology of F0 XX *Tg(amhy,EGFP)* males
221 showed key differences between fertile, subfertile, and hypotrophic testes (Fig 3A). Fertile
222 males had normal testis histology with visible mature spermatozoa. The subfertile male testis
223 lacked spermatozoa, instead containing meiotic spermatocytes and immature round spermatids
224 concordant with its reduced fertility. Histology of the hypotrophic testes showed the germ cells
225 were still early undifferentiated spermatogonia. This phenotypic variation may be a result of
226 variable *amhy* expression influenced by transgene copy number and insertion location.
227 Sex-reversed XY *amhy*-KO females produced mature oocytes and became gravid, but
228 they were subfertile compared to wildtype females. To assess fertility, we crossed three F1 XY
229 *amhy*-KO females to wildtype XY males. These clutches all showed extremely low viability rates
230 (2% n=43, 4% n=51, and 6% n=63) (S2 Table). One of the three F1 fish was crossed four
231 additional times and showed improvement in viability with the subsequent crosses. The viability
232 rates of the fourth and fifth cross were 78% (n=100) and 79% (n=89) respectively, though this is
233 still lower than the average viability of eggs from nine wildtype females (85% n=857) (S1 Table
234 S1,S2 Table). Three days after fertilization, 50 of the 148 viable F2 eggs had arrested
235 development. We were able to genotype 48 of the failed embryos. 36 of the 48 arrested
236 embryos were YY and carried both the paternally transmitted Y chromosome (Y^{+}) and the
237 maternally transmitted *amhy*-KO Y chromosome (Y^{KO}) (Fig 4D). The remaining embryos were
238 reared to adulthood and 92 were genotyped for their sex chromosome complement. No adult
239 $Y^{+}Y^{KO}$ fish were observed, indicating that the YY genotype is embryonic lethal due to the
240 missing X chromosome (Fig 4A, Fig 4B). XY^{KO} females were found to transmit the X and Y^{KO}
241 chromosome with equal frequency, indicating there was not any biased transmission of the X or

242 Y chromosome during female meiosis (36 $Y^{+}Y^{KO}$ embryos out of 148 total does not deviate from
243 a 1:3 Mendelian ratio; chi-squared = 0.0360; p = 0.8494; of the 92 adult F2s genotyped 36 XX,
244 27 XY^{+} , and 29 XY^{KO} does not deviate from the expected 1:1:1 ratio; chi-squared = 1.457; p =
245 0.4827).. We also measured fertility in an F2 cross which contained sex reversed XY^{KO} females
246 and wildtype XX female siblings. We crossed 11 F2 females (5 XX and 6 XY^{KO}) with wildtype XY
247 males. The clutch size did not differ significantly between XY^{KO} and XX females (Fig 4C, S3
248 Table). However, the viability rate was substantially lower in the F2 XY^{KO} females, similar to the
249 F1 generation (Fig 4C, S3 Table). Two F2 females were also eggbound and were unable to be
250 stripped of eggs. Both eggbound females were XY^{KO}, and no eggbound XX females were
251 observed at the time crosses were performed.
252

253 **Male nuptial coloration is present in both sex reversed genotypes.**

254 Male nuptial coloration is one of the most prominent sexually dimorphic characteristics in
255 threespine stickleback. During their breeding season, males from many stickleback populations
256 develop red throats and dark blue eyes and bodies [82]. To investigate the separate
257 contributions of gonadal and genotypic sex on this trait, we compared coloration in mature sex
258 reversed XX *Tg(amhy,EGFP)* males and XY *amhy*-KO females to wildtype XX and XY fish (Fig
259 5). Neither XX *Tg(amhy,EGFP)* males nor XY *amhy*-KO females appeared to fully recapitulate
260 wildtype XY male coloration, but both were distinct from wildtype XX females (Fig 5A). XX males
261 had blue coloration on their eyes and bodies, but none were as dark as completely colored XY
262 males. XY females were varied in appearance, but some had discernably blue eyes and
263 darkened bodies not seen in XX females. We measured the proportion of body area that was
264 blue or dark for each genotype (S8 Fig, S4 Table). As red throats are not prominent even in
265 wildtype males under our laboratory conditions, we were not able to quantify this trait. Both
266 proportion of dark and blue body area showed wide variation within genotypes (Fig 5B). We saw
267 significantly more blue ($p < 0.0001$) but not dark coloration ($p = 0.1161$) in XY males compared

268 to XX females. XX males were significantly less blue (p = 0.0003) and dark (p = 0.0007) than
269 XY males. XY females were significantly more blue than XX females (p = 0.0348), but there was
270 no difference in darkness (p = 0.1074). Together, these findings show that male nuptial
271 coloration is influenced both by hormones produced by the testis and by sex chromosome
272 genotype, but both male gonad differentiation and an XY genotype is needed to present full
273 male nuptial coloration.
274

275 **_amhy_ contributes to higher total _amh_ dosage early in development.**

276 Since Amh shows high specificity for its dedicated receptor, AmhrII, [28–30] we predicted
277 that *amhy* would be functionally constrained regarding coding sequence evolution and would
278 instead evolve novel function through regulatory changes. We investigated the degree of
279 sequence conservation within putative regulatory regions (2 kb upstream and downstream of
280 the coding sequence), of *amhy* relative to autosomal *amh*. We also compared sequence
281 similarity between *amh* and the orthologous *amh* in the ninespine stickleback (*Pungitius*
282 *pungitius*) which do not have an *amhy* (Fig 6, S5 Table). The divergence time between
283 threespine and ninespine stickleback is approximately 26 mya [83], similar to the 22 mya
284 divergence time between the threespine *amh* and *amhy* [20]. There was less sequence identity
285 between the coding sequences of threespine *amh* and *amhy* (0.780) than between threespine
286 *amh* and ninespine *amh* (0.879). Lower sequence identity despite shorter divergence time is
287 consistent with weaker purifying selection acting on the Y chromosome due to a lack of
288 recombination [84]. This was also supported by a higher overall dN/dS value between
289 threespine *amh* and *amhy* (0.780) than between threespine *amh* and ninespine *amh* (0.668),
290 though this pattern did vary across exons (S5 Table). Alternatively, reduced sequence identity
291 and elevated dN/dS could be due to positive selection acting on coding sequence changes to
292 *amhy*. The sequence identity of upstream and downstream regions was much lower between
293 threespine *amh* and *amhy* (0.365 and 0.376) than between threespine *amh* and ninespine *amh*

294 (0.595 and 0.660), indicating *amhy* has undergone significant regulatory evolution since its
295 duplication onto the Y chromosome, which may cause differences between *amh* and *amhy*
296 expression.

297 To determine whether expression of these genes differ throughout development, we
298 sequenced the total transcriptomes from prehatching embryonic stages 17 (early
299 somitogenesis, ~43 hpf), 20 (onset of pigmentation, ~73 hpf), and 23 (completion of yolk sac
300 circulation, ~122 hpf), stage 26 larvae (0 days post hatching (dph), around 200 hpf), as well as
301 larvae 4 and 8 dph [85]. The earliest identified difference between male and female threespine
302 stickleback is an increase in primordial germ cell count in females relative to males at 3 to 4
303 dph, followed by differences in germ cell morphology at 7 dph [86]. Sex determination should
304 begin sometime prior to this stage. We predicted that the unique regulatory architecture of *amhy*
305 resulted in earlier expression timing relative to *amh.* Thus, we predicted *amhy* would be
306 expressed at higher levels relative to *amh* early in development in order to initiate sex
307 determination. As the gonad differentiates, *amh* expression should increase relative to *amhy*
308 due to the canonical role of *amh* in male differentiation. This pattern has been observed in
309 Japanese flounder [15] and Patagonian pejerrey [13], which also have *amhy* SD genes. To
310 compare *amh* and *amhy* expression, we first scaled *amhy* read counts by the difference in
311 transcript length which is not accounted for by normalized read counts (S6 Table). We then
312 tested whether *amhy* expression was different from one half of autosomal *amh*, as males have
313 two copies of *amh* and one copy of *amhy*. Average expression of *amhy* was higher than one half
314 *amh* at stage 23 and all timepoints post hatching, but this difference was only significant at
315 stage 23 ($p = 0.0454$). We found *amhy* expression trended towards higher expression at later
316 developmental stages, consistent with a role in sex determination. However, this difference was
317 only significant between stage 20 and 4 dph ($p = 0.0398$, Tukey HSD = 0.0361). We then
318 hypothesized that male sex determination could be initiated by a higher overall dose of *amhy*
319 when expressed simultaneously with *amh.* We combined *amh* and transcript length adjusted

320 *amhy* normalized read counts at each stage and found total amh dosage was higher in males at
321 0 dph (p = 0.0448), 4 dph (p = 0.0347), and 8 dph (p = 0.0297) (S6 Table), across the time
322 where germ cell count diverges in males and females. Together, these results suggest that
323 increased total dosage of amh provided by *amhy* is key to its role in male sex determination.
324

325 **Sex differentiation genes are not differentially expressed between males and**
326 **females early in development.**

327 Following sex determination, we expected to see divergence in the expression of overall
328 male and female transcriptomes. However, principal component analysis of autosomal gene
329 expression indicated that male and female larvae had similar expression profiles. Autosomal
330 genes were clustered by developmental time rather than separating by sex at any stage of
331 development (Fig 7A). Only sex chromosomes showed clear separation by both sex and
332 developmental time (S9 Fig), since the X chromosome is expressed two-fold higher in females,
333 relative to males, and the Y chromosome is only expressed in males. The overall lack of sex-
334 specific expression on the autosomes suggests that many aspects of sex differentiation occur
335 well after the earliest noted phenotypic difference between males and females: the proliferation
336 of germ cells in the primordial gonad at 3 to 4 dph [86].

337 We examined whether any developmental stages had genes that were significantly
338 differentially expressed between males and females. Many male and female differentiation
339 genes are highly conserved across vertebrates [2] and should also be expressed during
340 development of the threespine stickleback. For instance, we expected differential expression of
341 key transcription factors canonically involved in differentiation, including the male biasing factors
342 *dmrt1* and *sox9b* or the female biasing factors *foxl2a*, followed by divergence of downstream
343 genes such as the aromatase enzyme *cyp19a1a* and the TGF-b hormones *amh* and *gsdf*. In
344 total, we found 455 differentially expressed genes (DEGs) between males and females on the

345 autosomes (S1 File). Key regulators of differentiation should be differentially expressed
346 throughout development and into adulthood in order to actively maintain gonadal fate [2].
347 However, 430 of the DEGs were only differentially expressed in a single stage (S1 File),
348 suggesting these genes do not play a substantial, ongoing role in sex differentiation.
349 Additionally, while we expected to see an increase in the number DEGs over time due to
350 activation of male and female specific gene networks, the number of DEGs was highest at stage
351 17 (156 DEGs), decreasing in later stages until a small increase from 4 dph (41 DEGs) to 8 dph
352 (65 DEGs) (S10 Fig). None of the canonical differentiation genes of interest were differentially
353 expressed between males and females at any timepoint examined in this study (Fig 7, Table 1).
354 Male differentiation genes *dmrt1* and *amh* and female differentiation genes *foxl2* and *cyp19a1a*
355 were differentially expressed in adult gonads of both wildtype and sex reversed fish shown by *in*
356 *situ* hybridization (Fig 2, S4 Fig, S7 Fig), indicating their function in differentiation are conserved.
357 Of the identified DEGs, only a small handful have known associations with gonadal function,
358 development, or differentiation. Two genes associated with germ cell specification and
359 maintenance [87], *ddx4* and *piwil1*, showed female biased expression at 8 dph (Fig 7C).
360 Interestingly, *amhrII,* which shows female biased expression in embryonic mouse gonads [88],
361 was also expressed more highly in females at 8 dph. Although *cyp19a1a* was not differentially
362 expressed, the steroidogenic enzyme *hsd17b1*, which plays a role in estrogen synthesis [89],
363 showed female biased expression at 8 dph. This gene acts as the SD gene in *Seriola* fishes [90]
364 and is upregulated in ovaries of Siberian sturgeon before the activation of *foxl2* or *cyp19a1a*
365 [91]. A lack of differential expression in many of these key genes indicates that gonad
366 differentiation occurs after 8 dph.
367 We identified some other DEGs that have known reproductive functions in other
368 vertebrates but do not have clear connections to sex differentiation and are only differentially
369 expressed at a single timepoint. Gonadotropin-releasing hormone II receptor (LOC120811940)
370 has known roles in the stimulating steroidogenesis in both testes and ovaries across mammals

371 [92] and had male biased expression at stage 17 (logFC = 2.74, adjusted P = 1.6E-3). TGF-beta
372 3 hormone is expressed more highly in male mice during gonadogenesis [93], and a TGF-beta 3
373 proprotein like gene (LOC120807995) was expressed slightly higher in females at stage 17
374 (logFC = -0.63, adjusted P = 0.042). *Piwil2*, another germ cell associated gene [87], was
375 expressed higher in males at stage 20 (logFC = 1.71, adjusted P = 4.0E-3). *Cdc25b* is
376 expressed at low levels in mouse ovaries and testes [94] and was male biased at stage 23
377 (logFC = 0.52, adjusted P = 0.012). Separin/separase (*espl1*) has known roles in mitotic and
378 meiotic chromosome segregation [95] and was expressed at higher levels in 8 dph females
379 (logFC = -0.56, adjusted P = 1.4E-4). Additional work will be necessary to understand what
380 function, if any, these genes have in threespine stickleback gonad development.
381

382 # Discussion

383 ### *amhy* is the sex determination gene in threespine stickleback fish.

384 Our findings demonstrate that *amhy* is the SD gene in threespine stickleback, as it is
385 both necessary and sufficient for sex determination (Table 2). Independently derived *amhy*
386 genes have been functionally demonstrated to have a role in sex determination in three other
387 clades of teleost; however, threespine stickleback offers a novel perspective as their *amhy* is
388 more diverged, and genetic sex determination is more canalized in this species. Nile tilapia and
389 Japanese flounder have only one and nine SNPs, respectively, that differentiate their X- and Y-
390 linked copies of *amh* [15,16], and *amhy* in Patagonian pejerry shares 94% nucleotide identity
391 with its autosomal paralog [13]. In all three of these species, genetic sex determination can be
392 overridden to varying degrees by temperature [96–98]. In contrast, the threespine stickleback,
393 *amh* and *amhy* only share 78% nucleotide identity (S5 Table). There is no evidence that
394 temperature can disrupt sex determination in threespine stickleback, and occurrences of sex
395 reversed or intersex stickleback in wild populations is rare [99,100]. This indicates that genetic

396 sex determination is highly canalized in threespine stickleback and less susceptible to
397 environmental signals that many other teleost species, making stickleback a robust model to
398 investigate how *amh* regulates gonadal development. Comparative studies across these taxa
399 will be invaluable for understanding how *amh* repeatedly evolves this novel function, and the
400 presence of an independently derived male associated *amh* duplication in the closely related
401 brook stickleback [22,40] makes the stickleback family an especially powerful tool for studying
402 the convergent evolution of *amh* as an SD gene.
403

404 **Potential mechanisms of sex determination in stickleback.**

405 Germ cell density has been shown to affect sex determination in several teleost species,
406 with the male fate associated with lower germ cell count and the female fate with a higher count.
407 Common lab zebrafish strains are undifferentiated gonochorists, where all individuals begin
408 ovary development, but the gonad transitions early in males to a testis [101]. Complete ablation
409 of germ cells causes zebrafish to undergo male development [102], and a threshold of germ
410 cells at the time of gonadal differentiation is necessary to sustain ovary development [103]. *O.*
411 *latipes*, like sticklebacks, are differentiated gonochorists where either testis or ovary
412 development begins from a common undifferentiated primordium [104]. Ablation of germ cells in
413 XX *O. latipes* causes female-to-male sex reversal [105], and overproliferation of germ cells in
414 XY fish causes male-to-female sex reversal [106]. The association of germ cells with sex has
415 also been observed outside of teleosts in the red eared slider turtle (*Trachemys scripta elegans*)
416 which has temperature dependent sex determination. Embryos incubated at female promoting
417 temperatures have higher germ cell counts than those incubated at male promoting
418 temperatures, and depleting germ cells at intermediate temperatures biased the sex ratio
419 towards males [107]. Even after primary sex determination, germ cell depletion in mice [77] and
420 rats [108] leads to masculinization of the ovary, which produces Sertoli-like cells and
421 seminiferous tubule-like structures before its eventual degradation. This suggests the presence

422 of a widely conserved, ancestral mechanism in vertebrates by which germ cell density governs
423 gonad identity. A new duplication of *amh* could increase overall *amh* dosage, reducing germ cell
424 proliferation to co-opt this underlying mechanism and become a male determining gene.

425 Consistent with this mechanism, we found evidence that *amhy* contributes to higher amh
426 dosage in post hatching stages where differences in germ cell proliferation between males and
427 females are first observable in the developing gonad [86]. We also found increased expression
428 of germ cell specific genes (e.g. *ddx4* and *piwil1*) in females at 8 dph, corroborating previous
429 histological observations of increased germ cell proliferation in female stickleback gonads
430 beginning at 3 dph [86]. Overexpression of *Amh* in mice [77,109] causes reduced germ cell
431 count and gonad size in males and females, and loss of *Amh* alters primordial follicle
432 recruitment in females [110]. Similar findings have also been observed in chicken [78,111].
433 Studies misexpressing *amh* in telesots have primarily focused on sex determination; however,
434 gonadal hypertrophy observed in *amh* knockouts in other teleosts [32,34] alongside gonadal
435 hypotrophy with a lack of mature germ cells observed in some XX *Tg(amhy,EGFP)* males in this
436 study demonstrate the conserved function of *amh* suppressing germ cell proliferation in
437 stickleback and other teleosts.

438 Somatic cells may also be affected by *amhy* in other ways. In mice, low concentrations
439 of Amh promote proliferation and growth factor production in somatic cells, but increased
440 concentrations induce apoptosis [112]. Altering somatic cell proliferation could lead to
441 differences in the levels of hormones and growth factors that they produce, shaping gonadal
442 development. While Amh is not necessary for initial gonadal differentiation, it is important to
443 maintaining Sertoli cell fate in fetal mice [113]. Estrogen production in somatic cells also plays a
444 major role in sex differentiation and ovary development in teleosts (reviewed in [114,115]). In
445 tilapia, Amh signaling directly inhibits *cyp19a1a* production via Smad transcription factors [116].
446 While we did not detect a difference in *cyp19a1a* expression between males and females in

447 embryos or larvae, it is expressed more highly in adult ovaries than in testes, so *amhy* could
448 play a reinforcing role later in development to suppress estrogen synthesis in males.
449 The evolutionary changes that have given rise to novel function of *amhy* in stickleback
450 sex determination remain unclear. While we do see substantial sequence divergence in the
451 putative regulatory regions of *amhy* relative to *amh*, we only detected a significant difference in
452 expression at a single developmental stage. As we are unable to isolate embryonic gonadal
453 tissue for expression analysis, our results in this study are limited to characterizing total
454 expression in the whole embryo. This likely reduces our ability to detect differences in the
455 expression of genes like *amh* and *amhy* which are restricted to a small population of cells.
456 Alternative approaches, like single cell RNA-seq, spatial transcriptomics, or HCR *in situ* will be
457 useful to survey gene expression in the early differentiating gonad. Still, we should not rule out
458 the significance of coding sequence evolution for *amhy*. In Nile tilapia, *amhy* expression is lower
459 than the X-linked *amh* throughout development, and misexpression of *amhy* but not *amh*
460 induces male sex determination [16]. This implies that the single missense SNP between *amh*
461 and *amhy* in tilapia is important to the function of *amhy* in sex determination. In Spotted knifejaw
462 (*Oplegnathus punctatus*), a Y-linked copy of *amhrII* shows higher affinity for binding *amh* than its
463 X-linked paralog [23]. In zebrafish which lack *amhrII*, *amh* may instead use the type II TGF-β
464 receptor *bmpr2a* [117,118]. Mutations that increase the stability of Amhy, increase its affinity for
465 the receptor, AmhrII, or promote interaction with a non-canonical receptor could also affect
466 gonadal development. Manipulating *amh* and *amhrII* could provide further insight into the
467 evolution of *amhy* and its mechanism of inducing male development. We would predict knockout
468 of *amh* or *amhrII* to result in over proliferation of germ cells and some level of male to female
469 sex reversal in XY fish as is seen in medaka *amhrII* mutants [32]. This would demonstrate that
470 germ cell proliferation regulated by the canonical *amh* signaling pathway can influence sex in
471 stickleback, making protein evolution or interaction with non-canonical receptors less
472 parsimonious avenues by which *amhy* has evolved its novel function. Misexpression of *amh* and

473 *amhy* using regulatory elements from the opposite gene (i.e. expressing the *amh* genic
474 sequence with *amhy* regulatory elements) or non-native promoters could also elucidate whether
475 coding sequence evolution is important to the function of *amhy*.
476

477 **Sex differentiation occurs later than anticipated.**

478 We observed no differential expression in canonical vertebrate sex differentiation genes,
479 including *dmrt1, sox9b, foxl2a,* and *cyp19a1a.* While the order and timing of expression varies
480 across taxa, these core genes are reliably differentially expressed between males and females
481 before the onset of morphological gonadal differentiation [119–121]. These genes show
482 expected dimorphic expression patterns in adult gonads, shown both by our *in situ* data as well
483 as gonadal transcriptomic data [122]. This indicates that there is some delay between the initial
484 establishment of germ cell differences between males and females and the later differentiation
485 of the primordial gonad into either a testis or ovary. Expression analysis of whole embryos and
486 larvae could obscure gonad specific changes in gene expression as previously discussed.
487 However, we did identify differential expression of *ddx4* and *piwi1l* which are highly germ cell
488 specific [87] as well as *hsd17b1* and *amhrII* which are not gonad specific [89,123] but show
489 early female biased gonadal expression in other species [88,91]. This demonstrates some
490 ability to detect sex differences in expression for significant genes. Female biased expression of
491 *hsd17b1* precedes differential expression of these canonical differentiation genes in sturgeon,
492 where *hsd17b1* is thought to increase estrogen, upregulating of *foxl2* and *cyp19a1a* in females
493 [91]. In stickleback, female biased *hsd17b1* expression may be a key difference between males
494 and females, initiating expression changes in canonical differentiation genes. Further analysis of
495 gene expression at later timepoints will be necessary to determine if this is the case.
496 We propose that sex determination in threespine stickleback occurs in two phases. In
497 the early critical period of sex determination, germ cell proliferation in the undifferentiated gonad
498 diverges between males and females due to the presence of *amhy* in males. Then, during the

499 sensitive period of gonadal differentiation, the difference in germ cell count between males and
500 females dictates gonadal fate, marking the end of the sex determination and the beginning of
501 differentiation. Unlike *Sry* in mammals which is expressed in a brief window and directly initiates
502 gonadal differentiation [124], *amhy* in stickleback appears to be expressed throughout this early
503 period of germ cell proliferation. These two phases of germ cell proliferation followed by gonad
504 differentiation are also present in other species with SD genes including Nile tilapia (reviewed in
505 [125]), and medaka (reviewed in [104]) as well as species without SD genes such as red eared
506 slider [107] where germ cell proliferation is affected by temperature. This suggests that this two-
507 phase system of differential germ cell proliferation followed by gonadal differentiation is broadly
508 conserved across vertebrates, but what combination of environmental and/or genetic factors
509 influences germ cell proliferation has changed between taxa. The ability of *amh* to immediately
510 integrate with this preexisting sex determination network through its existing function in
511 regulating germ cell proliferation along with possible reinforcing roles in regulating somatic cell
512 identity and estrogen synthesis would explain the prevalence of *amh* as an SD gene.
513

514 **Fertility of sex reversed threespine stickleback.**

515 Both XY *amhy*-KO females and XX *Tg(amhy,EGFP)* male sex reversed fish were fertile
516 in our study. Fertility of sex reversed mutants is not uncommon in other teleost species;
517 however, it is often observed in species with younger or less diverged sex chromosomes. In
518 these instances, the X and Y chromosomes contain a similar complement of genes. In medaka,
519 the Y specific region is 280 kb and the only functional gene it contains is the sex determining
520 *dmrt1by* [12]. In Nile Tilapia, the sex determining region on linkage group 23 is 1.5 Mb and
521 contains 51 annotated genes, including the sex determining *amhy* [126]. In both species, sex
522 reversed fish are fertile and YY offspring are viable [11,127]. In contrast, the threespine
523 stickleback Y chromosome has a ~15 Mb non-recombining region [20]. Within this region, the Y
524 chromosome has lost half of the almost 1200 ancestral gametologs, causing inviability of YY

525 embryos, and has accumulated many Y-specific genes not present on the X chromosome [20].
526 Sex chromosome-specific gene content evolution could lead to improper expression in the
527 opposite sex, affecting gametogenesis. Given this divergence, the ability of both XY *amhy*-KO
528 females and XX *Tg(amhy,EGFP)* males to reproduce is surprising. In mouse, reduced fertility of
529 XY females is a result of meiotic errors between the X and Y chromosomes as well as the effect
530 of aberrant Y-chromosome genes in the ooplasm on early development (Reviewed in [128]). As
531 clutch size in XY females did not differ from XX siblings and some crosses from XY females
532 have normal viability, it seems unlikely that widespread meiotic failure occurs in XY female
533 stickleback. Furthermore, it is clear that Y chromosome transcripts or dosage differences from X
534 chromosome genes do not prevent embryo development. Threespine stickleback are batch
535 spawners that produce multiple clutches of eggs over a single breeding season [82]. If ovulated
536 eggs are not passed, they can become overripe and inviable [129,130]. Overripe eggs can also
537 harden and obstruct the fish, causing them to become eggbound. Many of the clutches from XY
538 *amhy*-KO females had this hardened, overripe appearance that is uncommon in our lab-reared,
539 wildtype fish. In addition, some XY females we attempted to cross had no cloaca dilation and
540 were eggbound. We suspect that subfertility of XY females is not due to an inability to produce
541 viable eggs, but due to an inability to pass these eggs once mature. Whereas wildtype fish can
542 pass eggs on their own and begin another cycle of ovulation, XY females retain these eggs until
543 they are manually removed. Repeated and frequent crossing would prevent overripe eggs from
544 building up and allow the harvest of freshly ovulated, viable eggs. Hormones produced by the
545 gonad and pituitary gland appears to play a role in egg maturation and overripening for
546 stickleback [130,131], so while XY females are histologically similar to XX females, variation in
547 hormone production could inhibit proper production and release of eggs.
548 The mammalian Y chromosome has several genes essential for spermatogenesis and
549 sperm development [132–136]. Single cell sequencing has shown that many Y-specific genes
550 are expressed throughout spermatogenesis in stickleback [137], but these genes are apparently

551 not essential for this process. Several XX *Tg(amhy,EGFP)* males from this study had testes with
552 many fully mature spermatozoa that were able to fertilize eggs and generate viable progeny at
553 similar rates to wildtype sperm. This raises a question of the importance of the Y chromosome
554 to fitness and reproduction. Testes from fertile XX males did not show an obvious reduction in
555 sperm number indicating that widespread meiotic arrest does not occur in XX males.
556 Stickleback are external fertilizers in which sperm competition frequently occurs [138]. Variation
557 in sperm morphology [139] and motility [140] can contribute to reproductive success, so there
558 may be differences in sperm function that our *ex vivo* fertilization assays do not capture. Some
559 XX *Tg(amhy,EGFP)* males did have hypotrophic testes with a reduction in identifiable germ
560 cells, but since this phenotype was not universal, we suspect that variation in transgene copy
561 number and insertion location led to overexpression of *amhy* in these fish. The germline
562 *Tg(amhy,EGFP)* offspring we produced will allow us to determine if this phenotypic variation
563 exists in a consistent genetic background.
564

565 **A four core genotypes stickleback model.**

566 Sex chromosomes impact a wide range of traits outside of fertility that are still critical to
567 fitness. By comparing XY males and XX females to sex reversed XY females and XX males, the
568 four core genotypes mouse model has allowed researchers to dissect the role of genotypic and
569 gonadal sex to a number of behavioral and physiological sex differences in mammals (reviewed
570 in [141,142]) including mating behavior [143] and parental care [144]. The creation of
571 reproductively mature XX males and XY females in this study offers a new vertebrate model to
572 study the separate contributions of gonadal sex and sex chromosomes to sexual dimorphism.
573 Many traits are sexually dimorphic in the threespine stickleback, including shape and
574 size of the head and body [43–46], bony armor features [43,44], and brain size [47,48] as well
575 as feeding behaviors [49,50] and boldness [51]. Male stickleback also show complex courtship
576 and mating behavior [52,53] and male-only paternal care [54], and females show a variety of

577 mate choice preferences [55–60]. Male nuptial coloration is a particularly interesting trait, as
578 strong coloration is beneficial for courtship [60,61], but has a cost of increased risk of predation
579 [62,63]. Therefore, sexually antagonistic selection would select for stronger, more conspicuous
580 coloration in males and inconspicuous coloration in females. Androgens, secreted from the
581 gonads, are shown influence nuptial coloration in stickleback [64]. These observations are
582 supported by the presence of nuptial coloration in XX males in our study, which lack all Y-linked
583 genes, but have functioning testes. In contrast, male nuptial coloration in XY females that lack
584 testes shows that there are also sex-linked genetic factors that contribute to nuptial coloration
585 independent of gonadal sex. Future research with the four core genotypes stickleback will
586 provide many insights into the genetic basis of sexual dimorphism and how sexually
587 antagonistic selection shapes the evolution of sex chromosomes.
588

589 # Methods

590 All experiments used lab-derived progeny from wild-caught threespine stickleback fish
591 from Port Gardner Bay (Washington, USA) and Japan Pacific Ocean (Akkeshi, Japan). All
592 procedures were approved by the University of Georgia Animal Care and Use Committee
593 (protocols A2021 07-031-Y3 and A2024 08-009-Y1). We collected fish from Washington State
594 over multiple years using Scientific Collection Permit numbers 21-122, 22-150, 23-147, and 24-
595 143. All experiments were performed using fish crossed and reared in laboratory conditions.
596 Fish were maintained in 3.5 ppt Instant Ocean Sea Salt (Spectrum Brands, Blacksburg, VA,
597 USA) in reverse osmosis water at 18 °C and pH 8.0 and a summer photoperiod (16L:8D). After
598 hatching, fry were fed freshly hatched Grade A Brine Shrimp (Brine Shrimp Direct, Ogden, UT,
599 USA) twice daily.
600

601 **CRISPR/Cas9 knockout of *amhy***

602 We microinjected stickleback embryos following standard procedures [41], with the
603 addition of KCl to the injection mix at a final concentration of 0.2 M [145]. Cas9 protein was
604 purchased from QB3 MacroLab (University of California, Berkeley). Synthetic sgRNAs were
605 designed using CHOPCHOP [146–148] and purchased from Synthego: amhy_sgRNA_77r (5'-
606 GATCAGCTGCTGTCCATGCA-3') and amhy_sgRNA_600r (5'- GGTCCTCTCTCGTCTTCGTT -
607 3'). We combined Cas9 protein and sgRNA at a final concentration of 10 μM each and
608 incubated for at least ten minutes at room temperature to allow the ribonucleoprotein (RNP) to
609 form. The injection mix was made to a final concentration of 4 μM RNP.
610

611 **Synthesis of constructs and transgenesis**

612 Plasmids pBT2 [149], pUbi:Switch [75], and pCS-zT2TP [8] were kindly shared by Mary
613 Goll. Plasmid pT2AL200R150G [71] (referred to as pT2Xla.Ef1a:EFGP) was kindly shared by
614 Tyler Square and Craig Miller. We purchased a synthetic amhy,EGFP construct from TWIST
615 Bioscience (San Francisco, CA, USA). This construct consisted of a Kozak consensus
616 sequence (5'-GCCGCCACCATGG-3'), N-terminus flag tag, the threespine stickleback *amhy*
617 coding sequence, a P2A self cleaving peptide [73,74], EGFP, and an SV40 poly(A) sequence,
618 all flanked by 5' BamHI and 3' NotI restriction sites to facilitate cloning. We performed all
619 restriction digests following the manufacturer's guidelines (New England Biolabs). We isolated
620 all of the plasmids using a Monarch Plasmid Miniprep Kit (NEB #T1010) and gel purified all DNA
621 fragments using the Monarch Gel Extraction kit (NEB #T1020). DNA fragments were ligated
622 using T4 DNA Ligase following manufacturer recommended protocols (NEB #M0202). We
623 transformed all plasmids into DH10B competent cells (Thermo Scientific EC0113). All plasmids
624 were sequenced by Azenta Life Sciences (South Plainfield, NJ, USA) (S2 File).
625 We assembled each construct as follows (S6 Fig):
626 1. pT2Dre.Ubi:amhy,EGFP: The *D. rerio* ubiquitin promoter was excised from
627 pUbi:Switch and cloned into pBT2 using XhoI and BamHI. The synthetic amhy,EGFP

628 construct was excised from pTwist_amhy-P2A-EGFP and cloned into the
629 intermediate pT2Dre.Ubi backbone using BamHI and NotI.
630 2. pT2Dre.Ubi:EGFP: the *D. rerio* ubiquitin promoter was excised from pUbi:Switch and
631 cloned into pT2Xla.Ef1a:EGFP using XhoI and BamHI.
632 3. pT2Xla.Ef1a:amhy,EGFP: the synthetic amhy,EGFP construct was excised from
633 pT2Dre.Ubi:amhy,EGFP and cloned into pT2Xla.Ef1a:EGFP using BamHI and BglII.
634 4. pT2-5amhy2.5,Xla.Ef1a:EGFP: an 11.5 kb region of the Y chromosome containing
635 *amhy* along with 5 kb of upstream and 2.5 kb downstream DNA was excised from
636 bacterial artificial chromosome STB26-N21 from the CHORI-215 library [150] and
637 cloned into pBT2 using BamHI and XhoI. The Xla.Ef1a:EGFP cassette was excised
638 from pT2Xla.Ef1a:EGFP by digestion with XhoI and HpaI and ligated into the
639 intermediate pT2-5amhy2.5 plasmid following digestion with XhoI and SwaI.
640 We synthesized Tol2 mRNA using the mMessage mMachine SP6 Transcription kit
641 (Invitrogen AM1340) and purified the product with the MEGAclear Transcription Clean-Up Kit
642 (Invitrogen AM1908). We injected stickleback embryos were as in [41] with the addition of KCl to
643 a final concentration of 0.2 M [145]. All embryos were screened for EGFP expression five to
644 seven days after injections before hatching had occurred. We removed all embryos without
645 discernable somatic EGFP fluorescence.
646

647 **Genotyping and sanger sequencing**

648 We extracted DNA from fin clips or whole embryos using a HotSHOT isolation protocol
649 [151]. We performed all PCR reactions on an Analytik Jena Biometra Tone in a total volume of
650 20 µl using 0.8 µL of genomic DNA, 0.2 µM each primer, 0.2 mM each dNTPs, 0.5 units
651 DreamTaq DNA polymerase (Thermo Scientific EP), and 2 µl 10x DreamTaq Green Buffer with
652 20 mM $MgCl_2$. We genotyped fish for sex using the sex-linked marker *idh* [39] with the following
653 cycling conditions: 1 cycle of 95°C for 2 min; 30 cycles of 95°C for 30 s, 57.3°C for 30 s, and

654 72°C for 30 s; 1 cycle of 72°C for 5 minutes. All other reactions used: 1 cycle of 95°C for 2 min;
655 35 cycles of 95°C for 30 s, 60°C for 30 s, and 72°C for 30 s; 1 cycle of 72°C for 5 minutes.
656 Primer sequences for all reactions are listed in S7 Table. We purified the PCR product using a
657 Monarch PCR & DNA cleanup kit (NEB #T1030). All samples were Sanger sequenced through
658 Azenta Life Sciences (South Plainfield, NJ, USA).
659

660 **Phenotyping and crossing**

661 To phenotype gonads, we euthanized adult stickleback fish in 0.05% MS-222 buffered to
662 neutral. We dissected out the gonads and fixed one or both gonads for 24 to 48 hours in 10%
663 neutral buffered formalin. The remainder of the fish was preserved in 75% ethanol. The gonads
664 were processed, embedded in paraffin, sectioned at 5 µm, and stained with hematoxylin and
665 eosin by the University of Georgia College of Veterinary Medicine Histology Lab. We used a
666 Zeiss Axio Scope A1 microscope and Zeiss Axiocam 305 Color camera to capture all images at
667 the University of Georgia Biomedical Microscopy Core.
668 To make crosses, we euthanized mutant or wildtype male stickleback and gently
669 macerated testes in 500 µl of Hanks' Balanced Salt Solution. We stripped eggs from gravid
670 females and applied approximately 50 µl of sperm solution with a disposable transfer pipette.
671 We photographed adult stickleback with a Samsung Galaxy S22 under standardized lighting.
672 We quantified coloration using FIJI (v. 1.54p) [152]. We Measured total fish body area using the
673 SIOX: Simple Interactive Object Extraction plugin. We used the Threshold Color plugin to
674 measure blue (Y = 0 – 254, U = 100 – 255, V = 0 – 131) and dark (Y = 0 – 31, U = 0 – 255, V =
675 0 – 255) body area in masked images. Pixel counts are presented in S3 File. We calculated the
676 proportion of body area for each color and performed a beta regression for differences in means
677 in R (v. 4.4.1) and RStudio (v. 2024.04.2+764) with the packages betareg (v. 3.2-4) and
678 emmeans (v. 1.11.2-8), allowing dispersion to vary by genotype (color ~ genotype | genotype).
679

680 **Riboprobe synthesis**

681 We generated riboprobe templates for *gsdf, dmrt1, foxl2,* and *cyp10a1a* from cDNA from
682 adult gonads. We extracted total RNA from mature testis and ovary tissue using TRIzol Reagent
683 (Invitrogen 15596026) according to manufacturer's instructions. We synthesized cDNA using the
684 iScript cDNA Synthesis Kit (Bio-Rad 1708891) and amplified the targeted region for each gene
685 through PCR as described above (S7 Table). We cloned the PCR product into plasmid pJC53.2
686 (kindly shared by Kendall Clay and Rachel Roberts-Galbraith) after digestion with Eam1105I
687 (Thermo Scientific FD0244) as in Collins *et al*. 2010 [153]. We verified each riboprobe template
688 after cloning with sanger sequencing by Azenta Life Sciences (South Plainfield, NJ, USA). For
689 *amh*, we ordered a synthetic gene fragment from TWIST Bioscience (San Francisco, CA, USA)
690 containing a 307 bp region of the *amh* cds flanked by a 5' T3 promoter and 3' T7 promoter to
691 facilitate riboprobe synthesis (S2 File).

692 To synthesize riboprobes, we PCR amplified linear template from the appropriate
693 plasmid or used the synthetic gene fragment directly. We performed *in vitro* transcription from
694 these templates using T7 (New England Biolabs M0251S), T3 (New England Biolabs M0378S),
695 or SP6 (New England Biolabs M0207S) RNA polymerase according to manufacturer's
696 instructions, substituting 0.2 mM of UTP for DIG-labeled UTP (Roche 11209256910). We
697 purified riboprobes with a DNase treatment (New England Biolabs M0303S) and an ammonium
698 acetate precipitation.

699

700 ***In situ* hybridization**

701 We adapted a colorimetric *in situ* hybridization (ISH) protocol from Square, *et al.* 2021
702 [154]. We fixed the dissected gonads for 24-48 hours in 10% neutral buffered formalin. The
703 gonads were processed, embedded in paraffin, and sectioned at 5 μm by the University of
704 Georgia College of Veterinary Medicine Histology Lab. Unless otherwise stated, we performed

705 all steps in Lock-Mailer microscope slide jars in a volume of 9-11mL and at room temperature.
706 To deparaffinize, we warmed the slides in a 65°C incubator for five minutes, allowed them to
707 cool to room temperature, then washed the slides in Hemo-De once for 5 minutes then again for
708 10 minutes. We performed prehybridization washes indicated with an asterisk in a Tissue-Tek II
709 Slide Staining Station rather than Lock-Mailer jars: 100% EtOH for 5 minutes*, 80% EtOH for 10
710 minutes*, Milli-Q water for 10 minutes*, PBST for 5 minutes*, 15 ug/mL proteinase K in PBST
711 for 5 minutes, PBST rinse*, 4% PFA for 20 minutes, PBST twice for 10 minutes each*, 67°C pre-
712 heated hybridization buffer (50% formamide, 5X SSC, 0.1% Tween, 5mg/mL CHAPS, 0.1
713 mg/mL yeast RNA, 0.1mg/mL heparin, pH 6.0 with citric acid) twice for 5 minutes each, and pre-
714 heated hybridization buffer for 1 to 4 hours on a rotator at 67°C. We performed hybridization
715 with 100-500 ng/mL of riboprobe in hybridization buffer incubated overnight rotating at 67°C. We
716 stored hybridization solution at 20°C and reused up to 3 times.
717 Post-hybridization, we washed the slides 6 times with hybridization wash (50%
718 formamide, 5X SSC, 0.1% Tween) rotating at 67°C for 20-90 minutes each, totaling 5 to 6
719 hours. We rinsed the slides in MABT (maleic acid buffer with Tween) and washed them in MABT
720 for twice for 20 minutes each, first at 67°C, then at room temperature. We added blocking
721 solution (2% Blocking Reagent (Roche 11096176001) in MAB) to each slide, covered the slides
722 with parafilm, and incubated for 1 to 3 hours in a humidor. We poured off the blocking solution
723 and added 1:2000 anti-digoxigenin alkaline phosphate antibody (Roche 11093274910) in
724 blocking solution, covered the slides with parafilm, and left them in a humidor overnight at 4°C.
725 We performed five 20-50 minute post-antibody washes hybridization wash solution (50%
726 formamide, 5X SSC, 0.1% Tween, citric acid to pH 6.0) on a rotator for a total of three to four
727 hours, followed by an overnight MABT wash at 4°C.
728 Prior to coloration, we performed three 5-to-10-minute washes in NTMT (0.1 M NaCl, 0.1
729 M Tris pH 9.5, 0.05 M MgCl2, 0.1% Tween). We moved the slides into coloration solution
730 (blocking solution plus 25 ug/mL NBT and 175 ug/mL BCIP) and incubated 2 to 30 hours

731 covered to block light. We removed the slides from coloration solution once the color was stable
732 in the positive control (*gsdf*), but before any background color was seen in the negative control
733 (sense *gsdf*). Once coloration was complete, we rinsed the slides with PBST and washed for 10
734 minutes in PBST. We fixed the slides in 4% PFA in PBS at 4°C for one to five days.
735 To prepare slides for mounting, we performed three 5-minute washes in PBST and three
736 5-minute washes in deionized water. We mounted and coverslipped the slides using Vectashield
737 antifade mounting medium with DAPI. We used a Zeiss Axio Scope A1 microscope and Zeiss
738 Axiocam 305 Color camera to capture all images at the University of Georgia Biomedical
739 Microscopy Core.
740

741 **Sequence Alignments**

742 We retrieved sequences for *amh* (Gene ID: 120823390) and *amhy* (Gene ID:
743 120812167) from threespine assembly GAculeatus_UGA_version5 (GCF_016920845.1) and
744 *amh* (Gene ID: 119216504) from ninespine assembly fPunPun2.1 (GCF_949316345.1). We
745 performed all alignments and calculated sequence identity between *amh* homologues with
746 Muscle 5.1 [155] within Geneious Prime (v2024.0.5) using default parameters. We defined
747 intron and exon positions based upon the threespine *amh* sequence in each alignment. We
748 calculated dN/dS with the R package ape v5.8-1 [156] using the translation aligned coding
749 sequences of *amh* (XM_040183306.1)*, amhy* (XM_040167960.1), and ninespine *amh*
750 (XM_037469420.2). One additional base was included at the 5' end of exon 7 of the ninespine
751 *amh* cds in order to correct the predicted annotation which contains multiple premature stop
752 codons in this final exon. Alignment files are presented in S2 File. We generated Vistaplots
753 [157,158] using LAGAN [159] alignments and a 100 bp window size with a 70% sequence
754 identity threshold.
755

RNAseq

We staged embryos according to established stickleback developmental stages [85] and preserved the whole embryos in RNAlater Stabilization Solution (Invitrogen AM7021) following manufacturer guidelines and stored at -80 °C until analysis. We extracted RNA using TRIzol Reagent (Invitrogen 15596026) and the Direct-zol RNA Microprep Kit (Zymo R2062). We created sequencing libraries using the Illumina TruSeq Stranded mRNA Library Prep kit (20020594). We pooled the libraries from all samples and 150 bp paired end reads were sequenced on two lanes using a NovaSeq X Plus by Azenta Life Sciences (South Plainfield, NJ, USA). All of the samples were sequenced to an average of 34.7 M read depth (min 11.6 M, max 71.3 M, SD = 10.4 M) (S1 File). We trimmed raw reads for quality and sequencing adapters with Trimmomatic (v. 0.39) [160] using leading and trailing quality threshold of 3, a sliding window of 4 with quality threshold of 15, and minimum length cutoff of 36. We aligned paired and orphan reads to the threespine stickleback reference genome (GAculeatus_UGA_version5, NCBI RefSeq assembly GCF_016920845.1) using HISAT-3N [161] with default parameters except for reversing RNA strandedness (R for Read 1 and F for Read 2). All samples had an alignment rate between 66% and 87%, counting only uniquely mapped reads (S1 File). We generated Indexed BAM files of the alignments with Samtools (v. 1.17). We generated transcript counts against the NCBI annotation GTF file (release 100) for GCF_016920845.1 with HTseq (v. 2.0.2) [162] using HTSeq-count with default parameters except for reversing RNA strandedness (R for Read 1 and F for Read 2). We performed all remaining analyses in R (v. 4.4.1) and RStudio (v. 2024.04.2+764). We combined the counts from paired and orphaned reads for each sample and used DESeq2 (v. 1.44.0) [163] to generate normalized read counts and perform differential expression analysis. We identified DEGs using the standard workflow with stage and sex combined as a single factor. We used the contrast function to calculate log2 fold changes (logFC) and adjusted p values for differential expression between males and females at each

781 timepoint. We identified DEGs of interest using GO terms from the NIH gene2go database
782 (https://ftp.ncbi.nlm.nih.gov/gene/DATA/).
783
784 **Material Availability**
785 RNAseq data is available in the NCBI SRA under BioProject PRJNA1248589. Raw and
786 normalized read counts are available in the NCBI GEO under accession GSE296766. All scripts
787 are available at https://github.com/MTreasterUGA/Amhy-sex-determination. All plasmids are
788 available upon request.
789

790 # Acknowledgements

791 This work was funded by the National Science Foundation MCB 1943283 (M.A.W), the National
792 Institutes of Health 1T32GM142623 (M.J.T.), The University of Georgia Research Foundation
793 (M.J.T.), the Society for the Study of Evolution R.C. Lewontin Early Award (M.J.T.), and ARCS
794 Foundation (M.J.T.).
795 Research reported in this publication was supported by the National Institute of General Medical
796 Sciences of the National Institutes of Health under Award Number R01GM147312 (M.A.W). The
797 content is solely the responsibility of the authors and does not necessarily represent the official
798 views of the National Institutes of Health.
799 This study was supported in part by resources and technical expertise from the Georgia
800 Advanced Computing Resource Center, a partnership between the University of Georgia's
801 Office of the Vice President for Research and Office of the Vice President for Information
802 Technology.
803 The imaging data used in this publication was produced in collaboration with the Biomedical
804 Microscopy Core at the University of Georgia.

We thank Koichi Kawakami (National Institute of Genetics, Japan) for use of the Tol2 elements in this study.

Declaration of Interests

The authors declare that there are no competing interests.

Figures

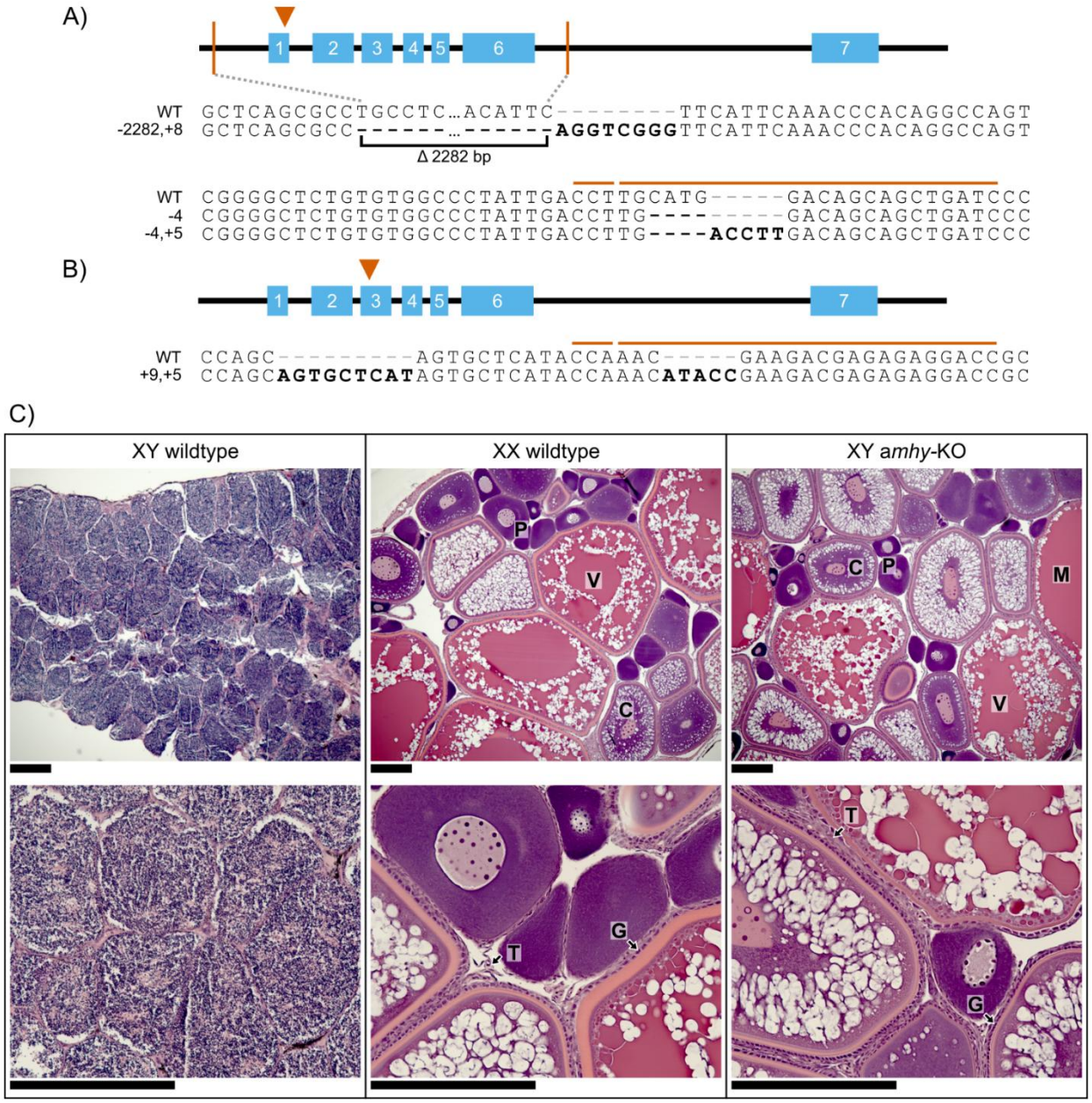

Fig 1. CRISPR/Cas9 knockout of *amhy* caused male to female sex reversal in F1 XY fish. We used CRISPR/Cas9 to target exon 1 (A) or exon 2 (B) of *amhy*. CRISPR target site and PAM sequence are indicated by orange lines above wildtype reference sequence. Mutations relative to wildtype are bolded. We identified four loss of function *amhy* alleles in F1 progeny. One allele (-2282,+8) deleted the first six exons of *amhy*. Other alleles featured small frameshift indels. C) We identified male to female sex reversal using gonad morphology and histology. Ovaries in XX wildtype and XY *amhy*-KO fish feature oocytes throughout multiple stages of development. P – primary oocyte, C – cortical alveolus stage V – vitellogenic stage, M – Mature oocyte, G – Granulosa cells, T – Theca cells. Scale bars = 200 µm.

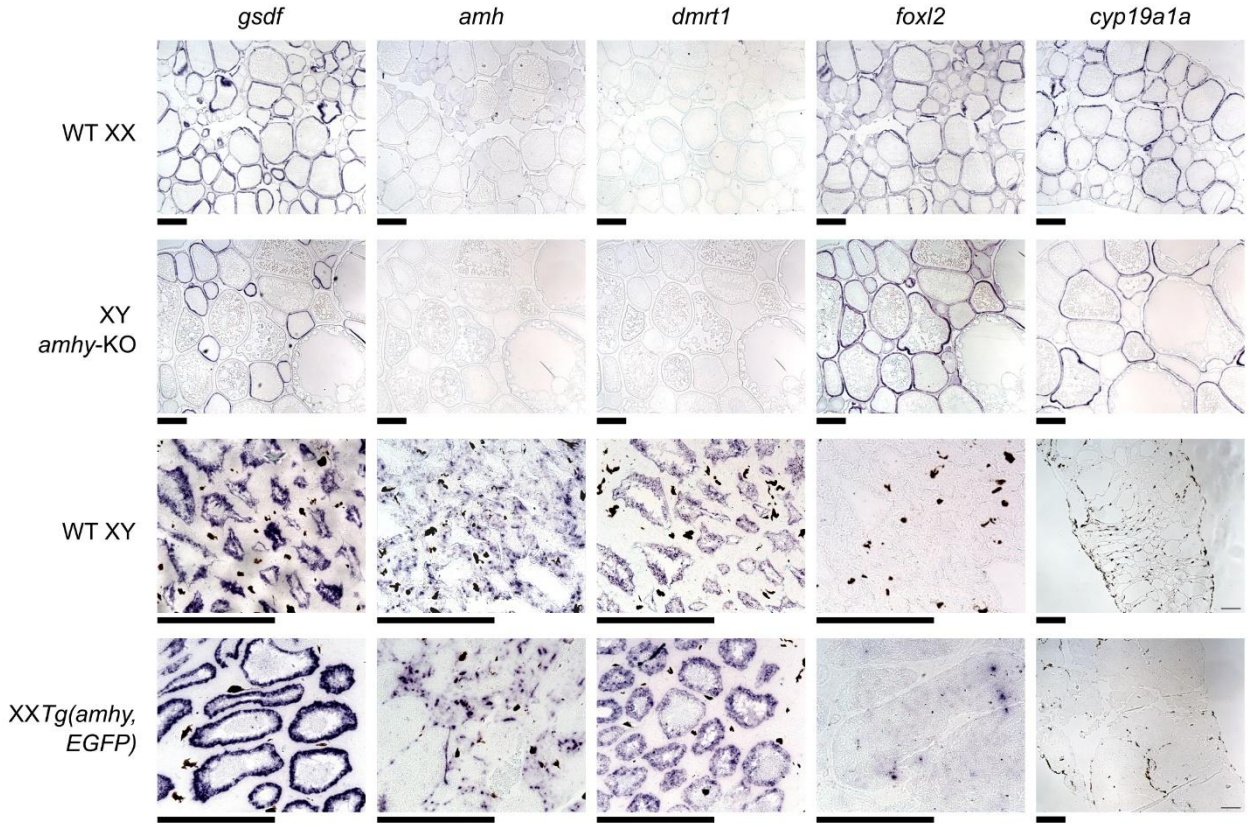

Fig 2. Gene expression in sex reversed gonads resembles expression in wild type gonads. *In situ* hybridization of gonadal genes in wildtype and sex reversed stickleback gonads. A positive control gene *gsdf* was expressed in somatic cells of both testes and ovaries. Wildtype XY and sex reversed XX testes show strong expression of male differentiation genes *amh* and *dmrt1* but not female differentiaiton genes *foxl2* and *cyp19a1a*. Wildtype XX and sex reversed XY ovaries strongly express female differentiation genes but not male differentiation genes. Scale bars = 200 μm.

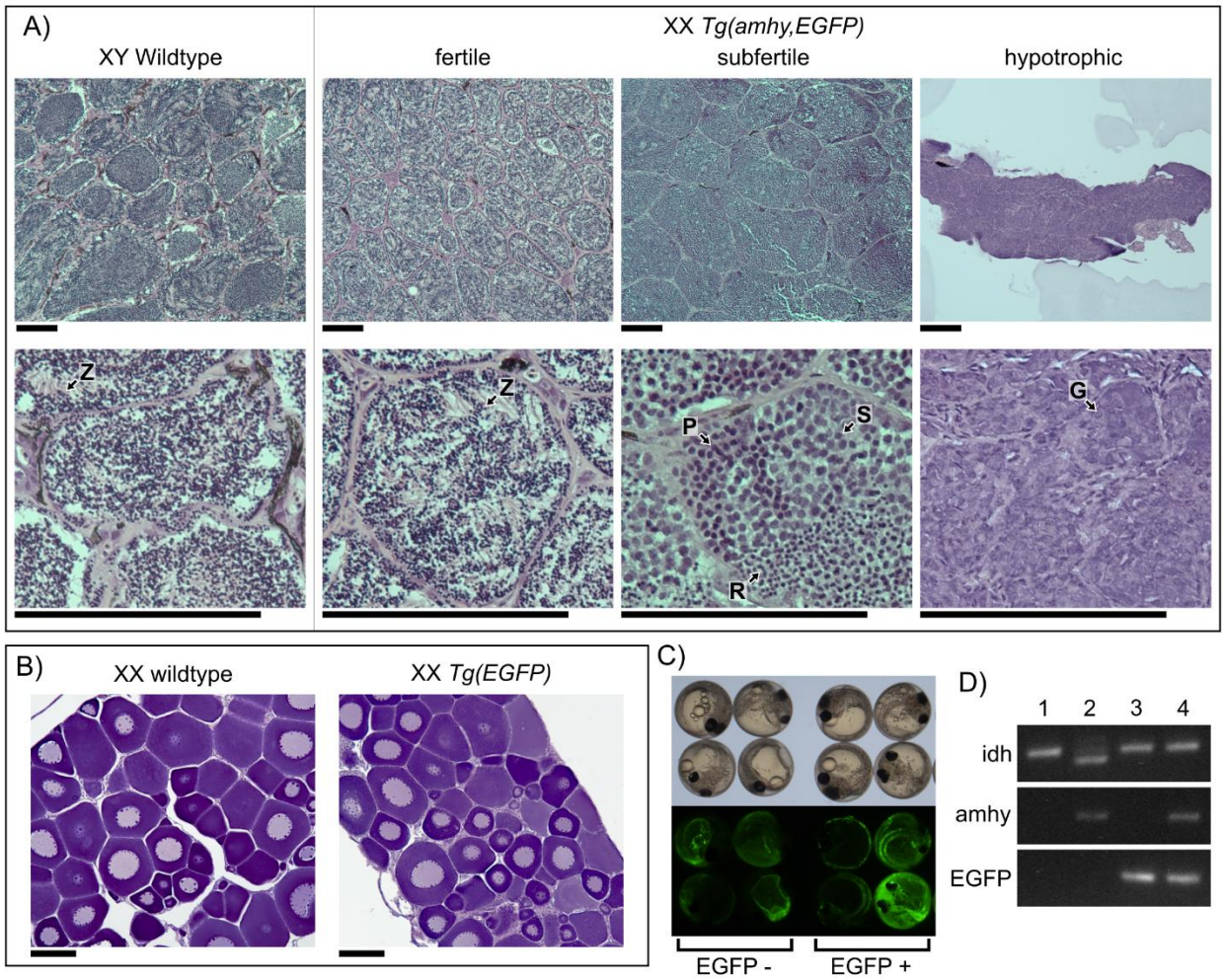

Fig 3. XX fish with an *amhy* transgene exhibit female to male sex reversal. A) XX *Tg(-5amhy3.5,Xla.Ef1a:EGFP)* fish developed testes with varying cell composition. Fertile fish had testes with clearly defined cysts of mature sperm as is found in wildtype fish. The subfertile testis had meiotic spermatocytes and immature round spermatids while hypotrophic testes had only undifferentiated spermatogonia. G – spermatogonia, P – primary spermatocyte, S – secondary spermatocyte, R – round spermatid, Z – Spermatozoa Scale bars = 100 μm. B) Control XX *Tg(Xla.Ef1a:EGFP)* fish developed ovaries identical to wildtype XX counterparts. Scale bars = 100 μm. C) Embryos injected with pT2-5amhy3.5,Xla.Ef1a:EGFP seven days after fertilization under bright field (top) and EGFP excitation (bottom). Embryos positive for transgene integration show somatic EGFP expression. We removed embryos with no EGFP expression or EGFP expression only in the yolk, which indicates the yolk was injected rather than the blastomere [41]. D) We used PCR of the sex-linked marker *idh* to genotype XX and XY fish. PCR of EGFP and *amhy* show the presence of the associated transgene. 1 – wildtype XX, 2 – wildtype XY, 3 – XX *Tg(EGFP)*, 4 – XX *Tg(amhy,EGFP)*.

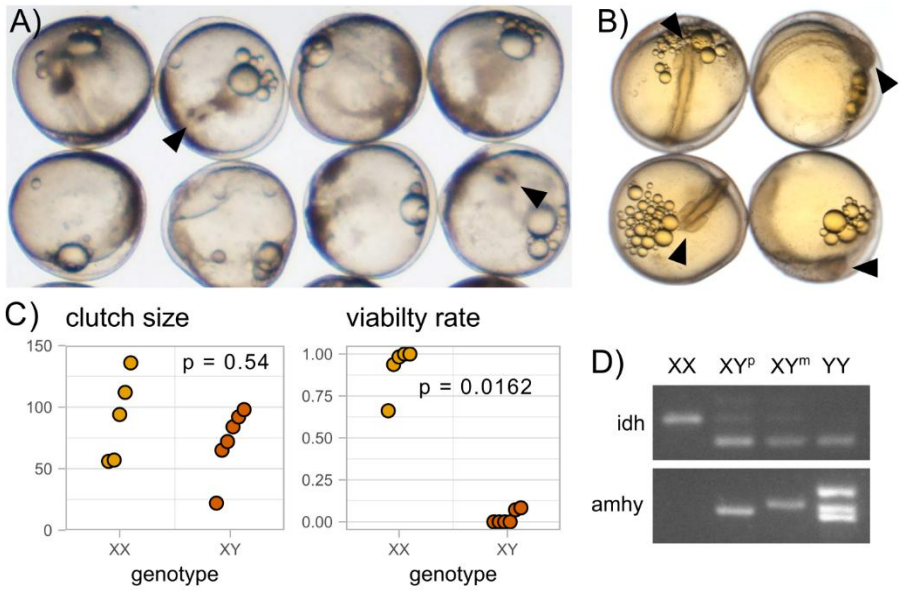

Fig 4. XY *amhy*-KO females can reproduce and transmit an X or Y chromosome. YY embryos (A) at 48 hours post fertilization show arrested development compared to wildtype embryos (B). Arrowheads denote anterior end of body axis. C) F2 XX and XY *amhy*-KO female siblings do not show a significant difference in clutch size (wilcoxon test, $p = 0.54$). Clutches from XY *amhy*-KO females have a significantly lower viability rate than those from XX female siblings (Wald z-test of beta regression coefficients, $z = -2.405$, $p = 0.0162$) . D) PCR of the sex-linked marker IDH shows the absence of the X chromosome in YY embryos. Both the paternal (wildtype) and maternal (+9,+5) loss of function alleles can be detected in XY offspring. YY embryos show the presence of both amhy alleles as well as a third band, likely a heterodimer of the maternal and paternal amplicons.

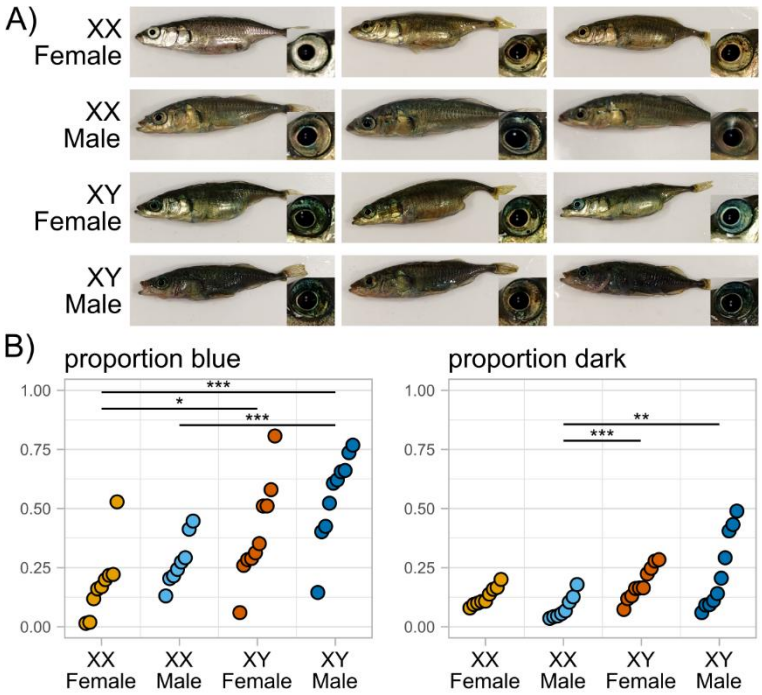

Fig 5. Both male and female sex reversed stickleback show partial male nuptial coloration. A) Representative images of wildtype XX females and XY males and sex reversed XX *Tg(amhy,EGFP)* males and XY *amhy*-KO females. XX females are silver and may darken slightly when gravid. XY males have dark blue eyes and bodies and red throats. Sex reversed XX males and XY females show intermediate aspects of male nuptial coloration. B) Proportion of body area that is blue or dark for each genotype. Differences in coloration between genotypes were tested using estimated marginal means from a beta regression with Wald z-tests and Tukey adjustment for pairwise comparisons (* $p < 0.05$, ** $p < 0.01$, *** $p < 0.001$) (S4 Table).

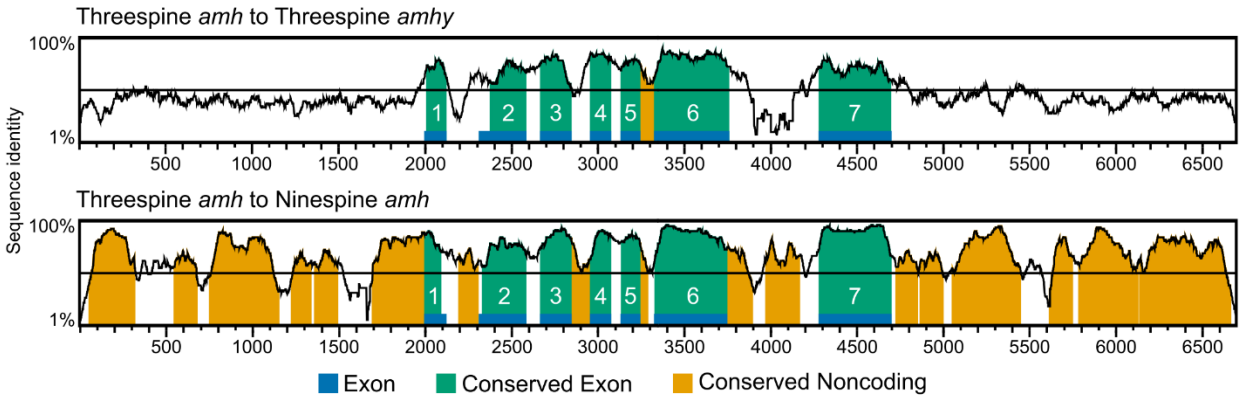

Fig 6. *amh* and *amhy* show no sequence conservation outside of the coding sequence. Vistaplots showing conserved sequence identity of threespine *amh* to threespine *amhy* (top) and to ninespine *amh* (bottom) with sequence identity on the y axis and nucleotide position of threespine *amh* on the x axis. Exon positions are indicated along the x axis in blue. Conserved exon and noncoding sequences share 70% sequence identity in a 100 bp window.

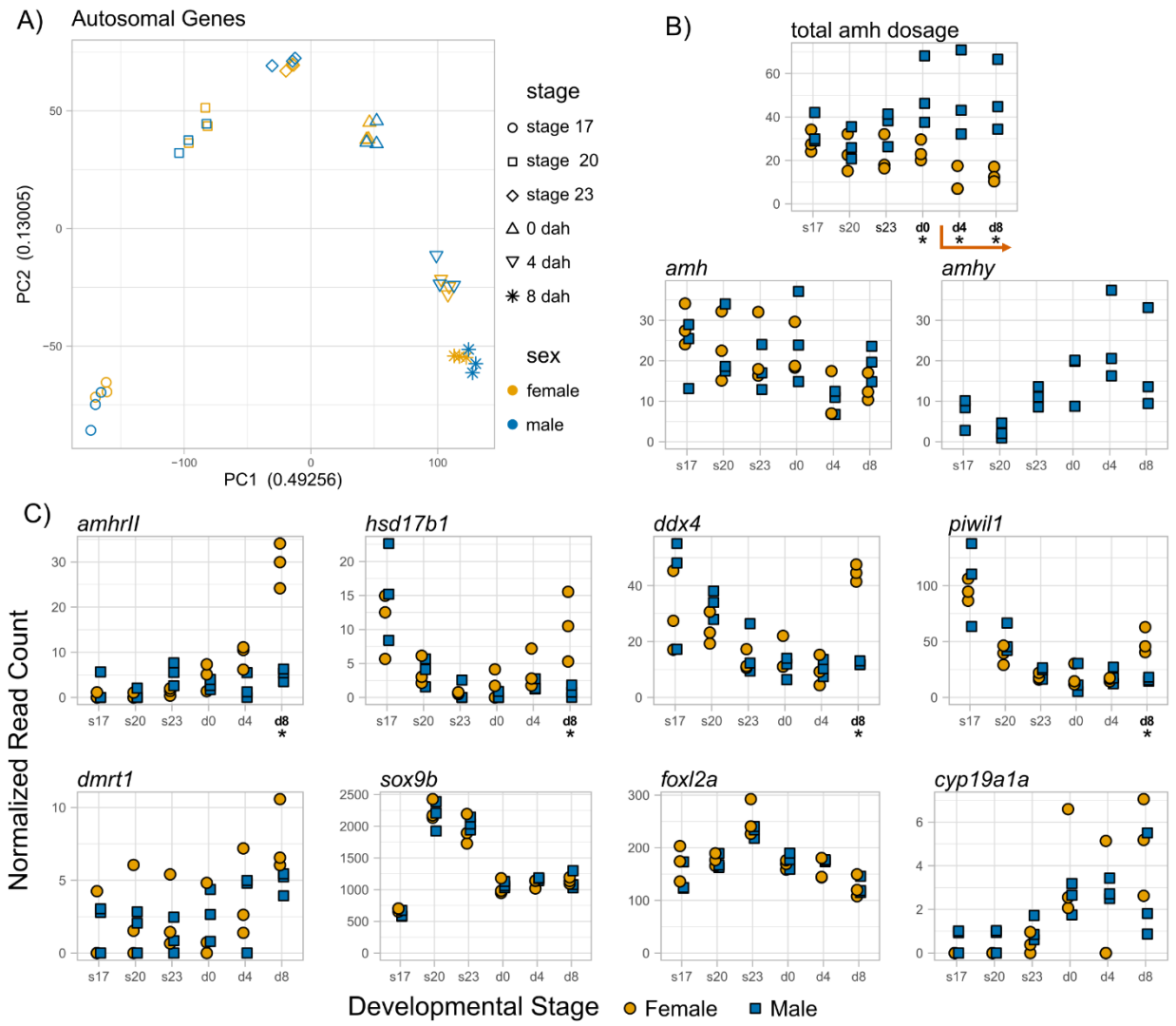

Fig 7. Expression of gonadal growth and differentiation genes in embryonic and larval stickleback. (A) PCA plots of normalized read counts for all genes cluster by stage rather than sex. (B) and (C) Normalized read counts of genes in embryonic stages 17, 20, 23, and larvae 0, 4, and 8 days after hatching. Stages with significant differences between males and females are marked with an asterisk and bolded ($p < 0.05$; Table 1, S6 Table). The orange arrow (B) indicates stages where differences in germ counts have been observed between males and females.

887 # Tables

888 **Table 1. Benjamini Hochberg adjusted P values for differential expression between males**
889 **and females.**

gene	gene id	stage 17	stage 20	stage 23	0 dph	4 dph	8 dph
amh	amh	1	1	1	1	1	1
amhrII	LOC120835457	1	1	0.341	1	0.609	**0.0313**
ddx4	ddx4	1	1	1	1	1	**0.00225**
piwil1	piwil1	1	1	1	1	1	**0.00245**
hsd17b1	hsd17b1	1	1	1	0.873	1	**0.0272**
foxl2a	foxl2a	0.832	1	1	1	1	1
cyp19a1a	LOC120811580	1	1	1	1	1	1
dmrt1	dmrt1	1	1	1	1	1	1
sox9b	LOC120827768	0.946	1	1	1	1	1
gsdf	gsdf	1	1	0.483	1	1	1
nr5a1	nr5a1a	1	1	1	1	1	0.983

890
891 **Table 2. Phenotypes of mutant stickleback from this study.**

Genotype	**N**	**Male (%)**	**Female (%)**
F0 XY *amhy* crispants	17	9 (53%)	8 (47%)
F1 XY *amhy*-KO	16	0 (0%)	16 (100%)
F0 XX *Tg(-5amhy2.5,Xla.Ef1a:EGFP)*	16	16 (100%)	0 (0%)
F0 XX *Tg(Xla.Ef1a:EGFP)*	10	0 (0%)	10 (100%)

892

Supporting Information

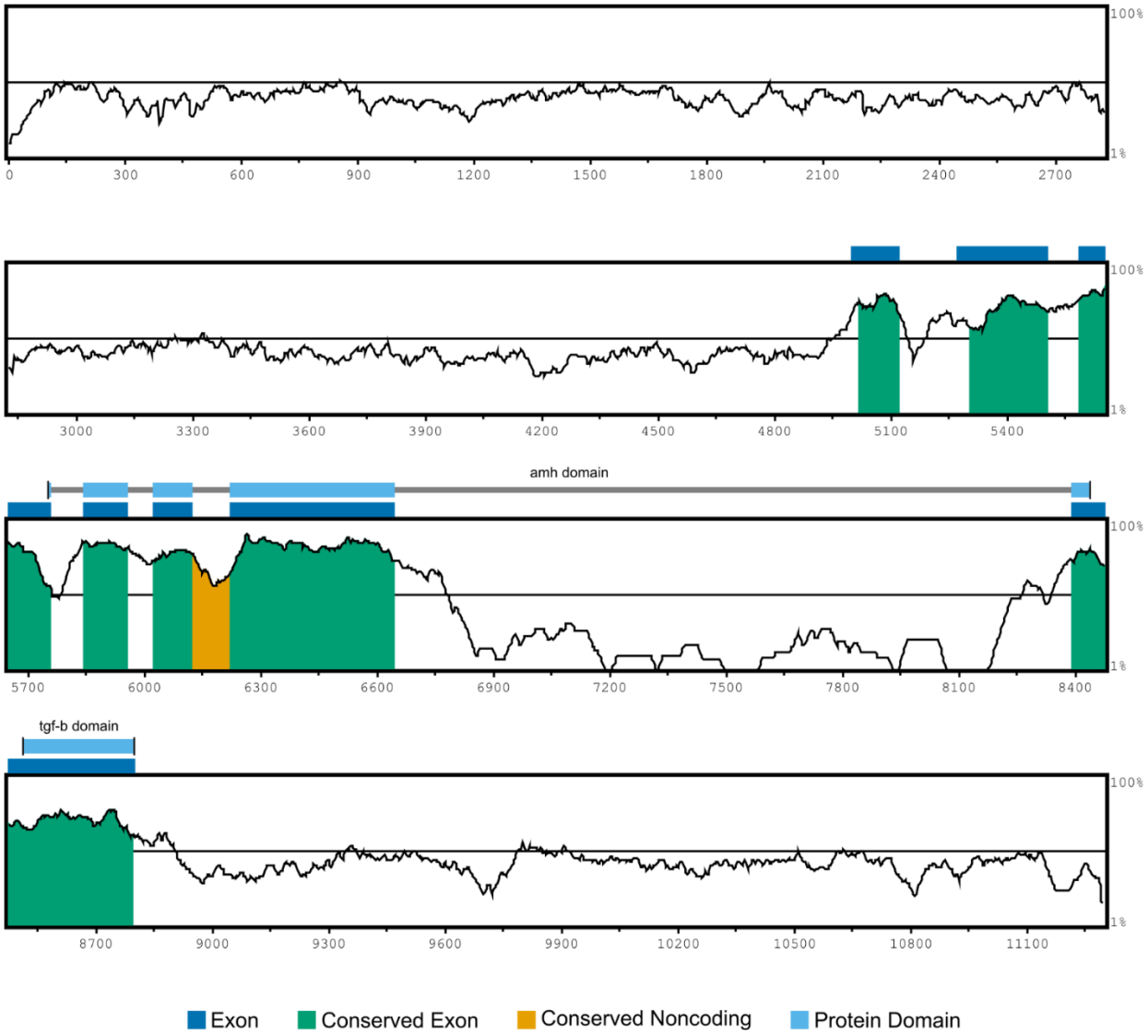

S1 Fig. Sequence conservation of the *amhy* transgene region with autosomal *amh*. Vistaplot showing conserved sequence identity of *amhy* to *amh* with sequence identity on the Y axis and base pair position of *amhy* on the x axis. Exon positions are indicated in dark blue, and the amh domain and TGF-β domain are indicated in light blue above the graph. Conserved sequences share 70% sequence identity in a 100 bp window.

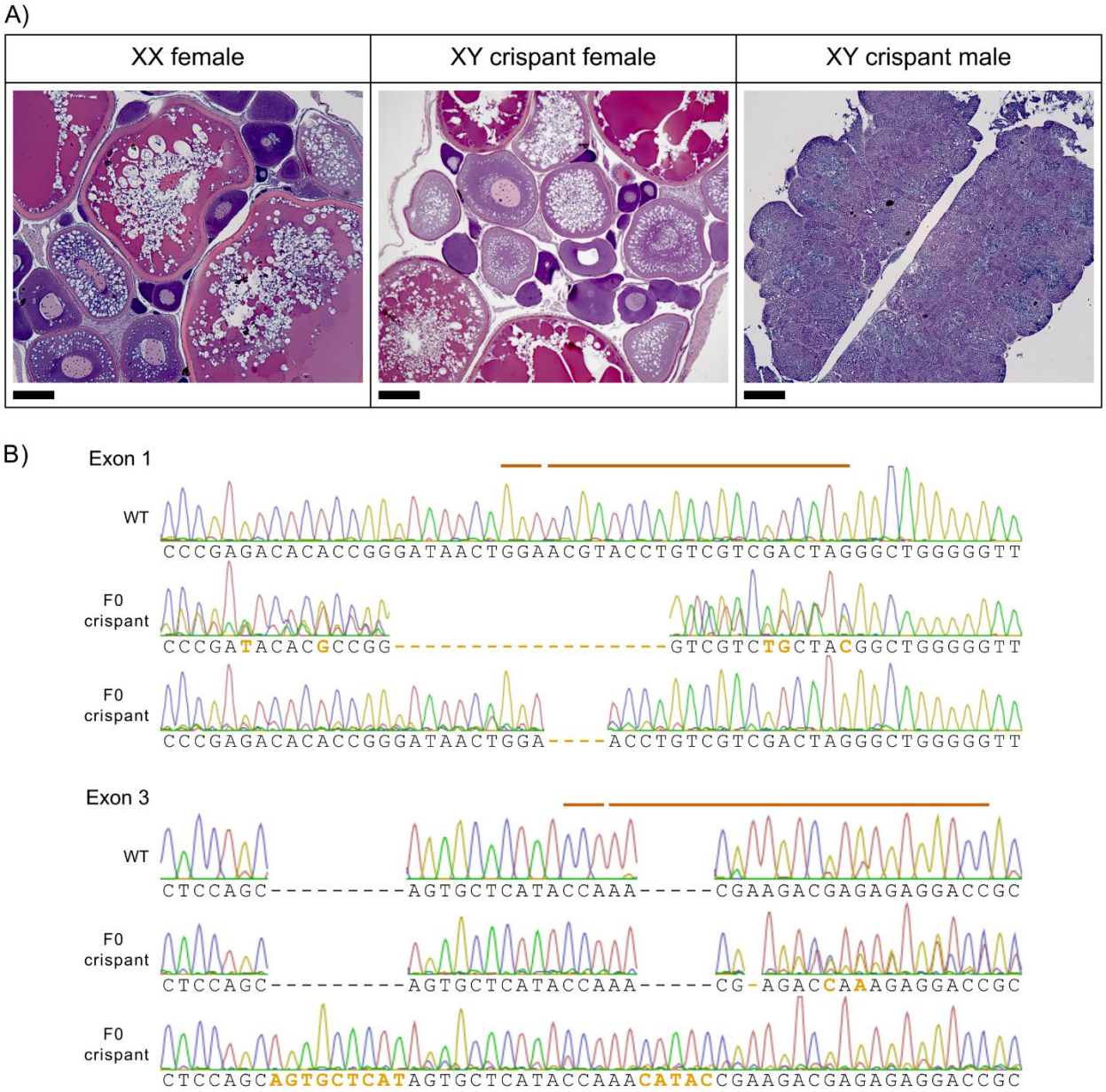

S2 Fig. F0 *amhy* crispants show genetic mosaicism and variable sex reversal. A) XY crispants developed as females with ovaries or males with testes. B) Sanger sequencing of exon 1 and exon 3 show various mutations relative to wildtype. Discordant chromatograms in crispants are indicative of mosaic mutations. Mutations are bolded in orange. CRISPR target site and PAM sequence are indicated by orange lines above wildtype reference sequence.

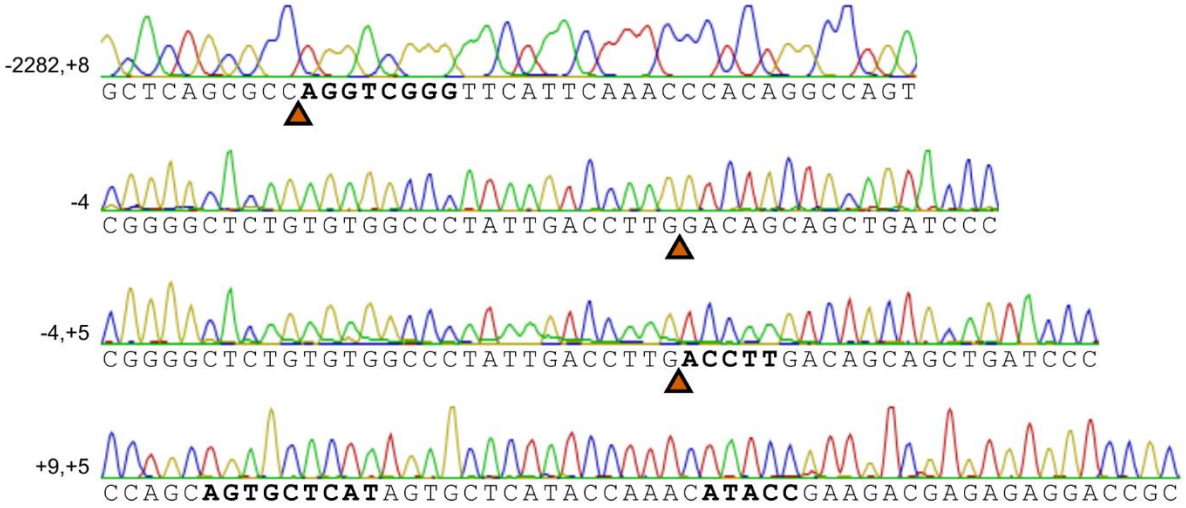

S3 Fig. Sanger sequencing of four F1 *amhy* mutant alleles. Inserted base pairs are bolded. Locations of deletions are indicated with red arrowheads.

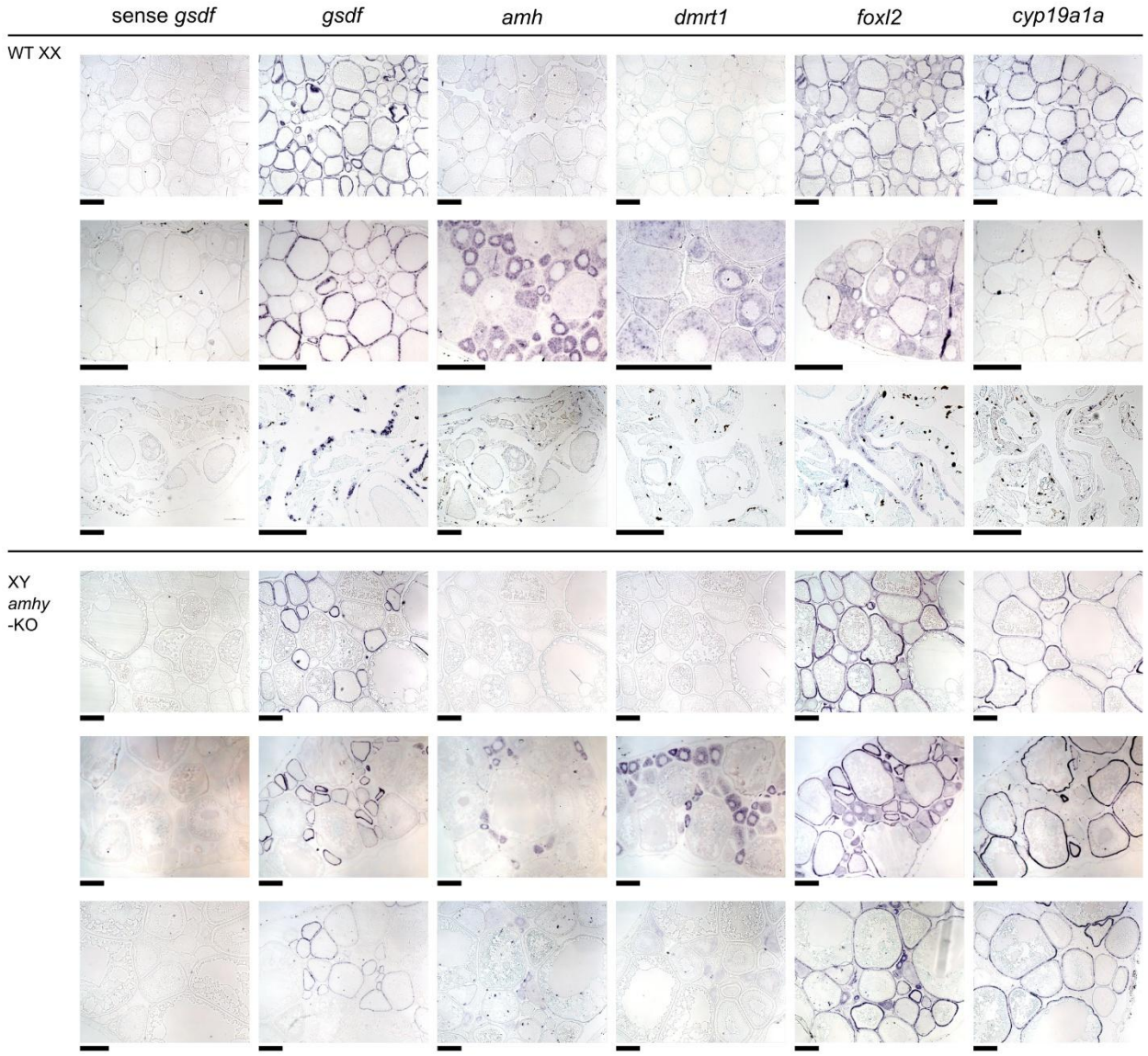

S4 Fig. Expression of gonadal genes in wildtype and sex reversed ovaries. *In situ* hybridization of gonadal genes in three biological replicates for wildtype XX ovaries and XY *amhy*-KO ovaries. Scale bars = 200 μm.

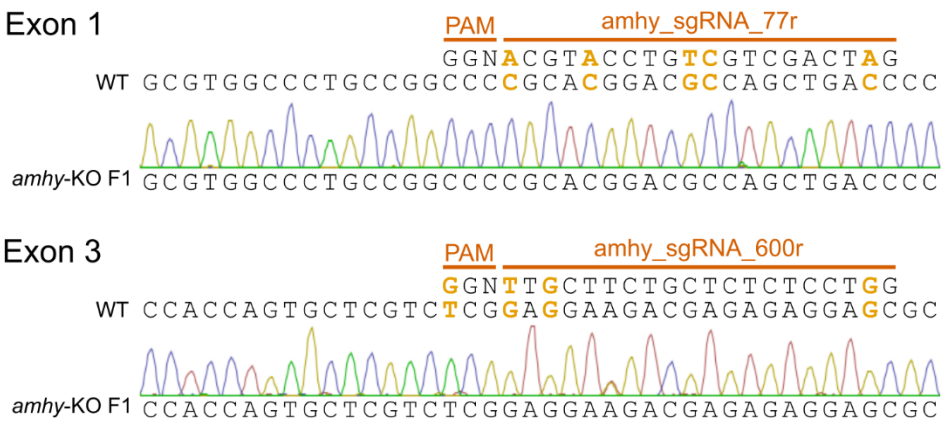

S5 Fig. CRISPR/Cas9 sgRNAs for *amhy* have multiple mismatches to their homologous site in *amh*. PAM and sgRNA sequences are shown above the reference sequence. Mismatched nucleotides are bolded in orange text. Sanger sequencing of sex reversed XY F1 *amhy*-KO fish showed no off-target mutations in *amh* in exon 1 (A) or exon 3 (B).

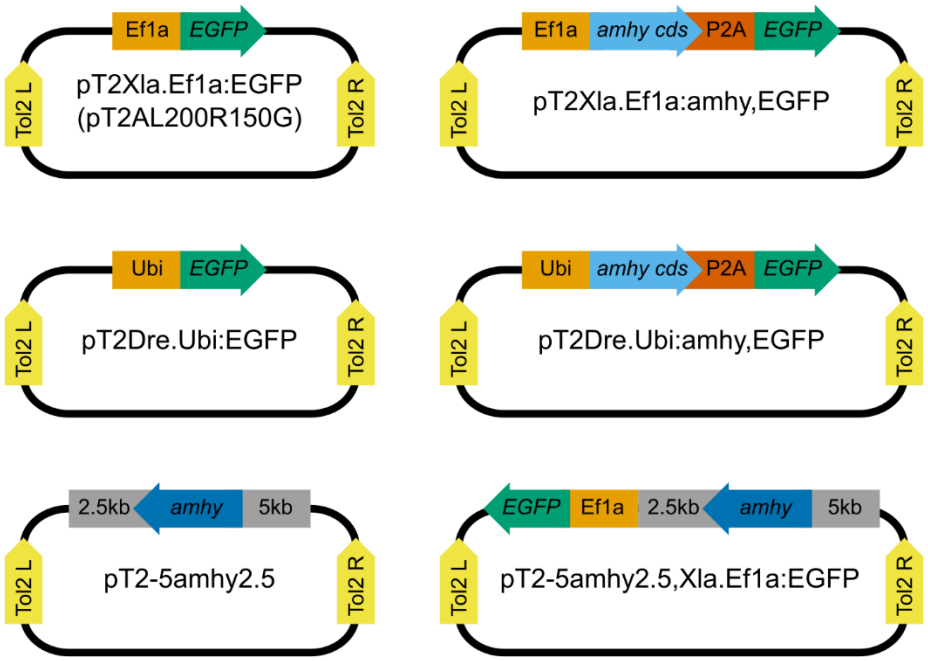

S6 Fig. Plasmid maps of transgenes constructed in this study. Transgenes used the ectopic *X. laevis* Ef1a or *D. rerio* Ubi promoter or the endogenous *amhy* promoter. Control transgenes express only EGFP. Other transgenes contain the *amhy* coding sequence or the full *amhy* sequence including introns. To screen for transgene integration, *amhy* transgenes include an EGFP joined to *amhy* with a P2A self-cleaving peptide or separate EGFP cassette. All transgenes are flanked by Tol2 transposon arms to facilitate transgene integration.

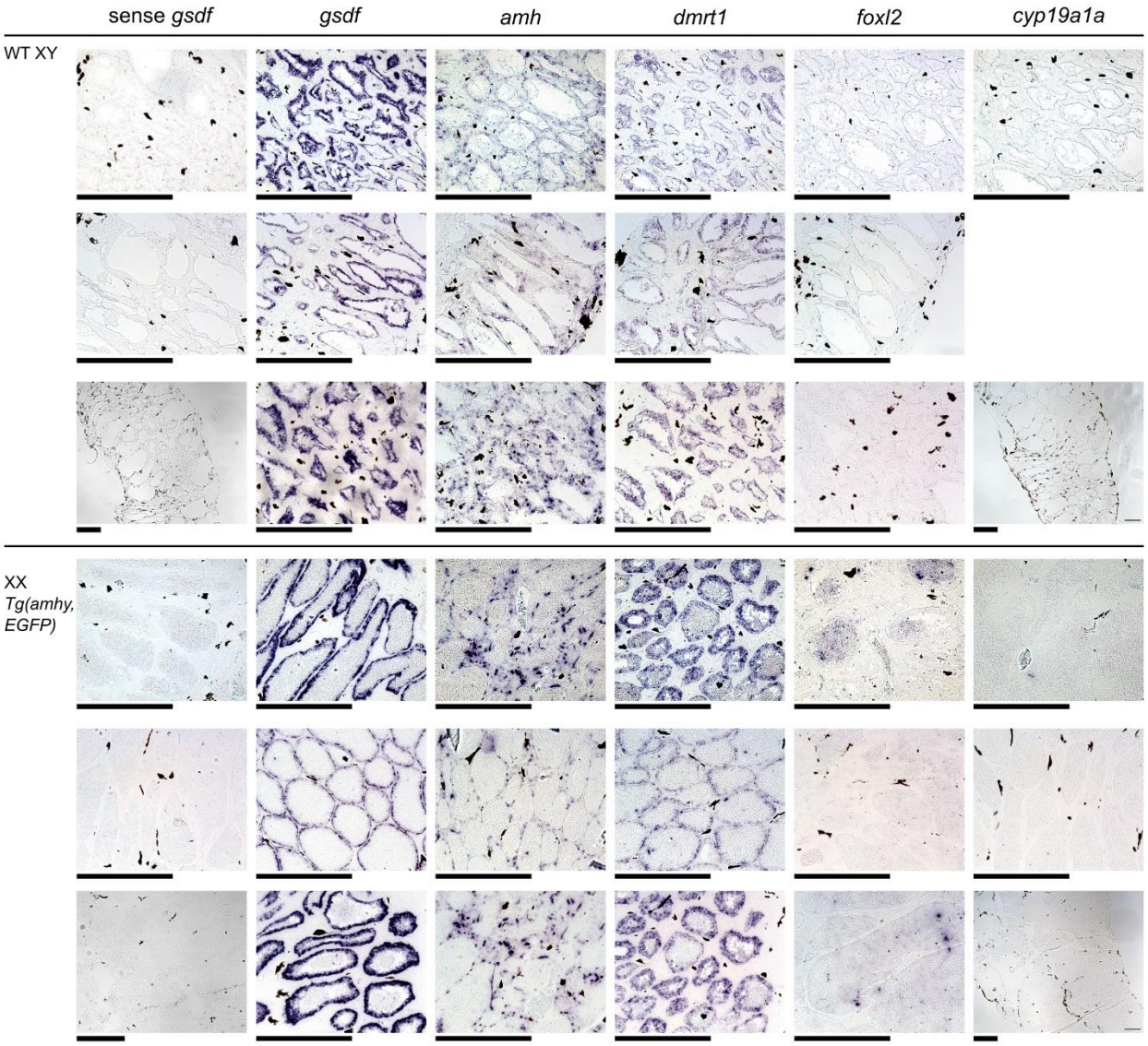

S7 Fig. Expression of gonadal genes in wildtype and sex reversed testes. *In situ* hybridization of gonadal genes in three biological replicates for wildtype XY testes and XX *Tg(amhy,EGFP)* testes. For one wildtype replicate, the tissue was lost during staining for *cyp19a1a*. Scale bars = 200 µm.

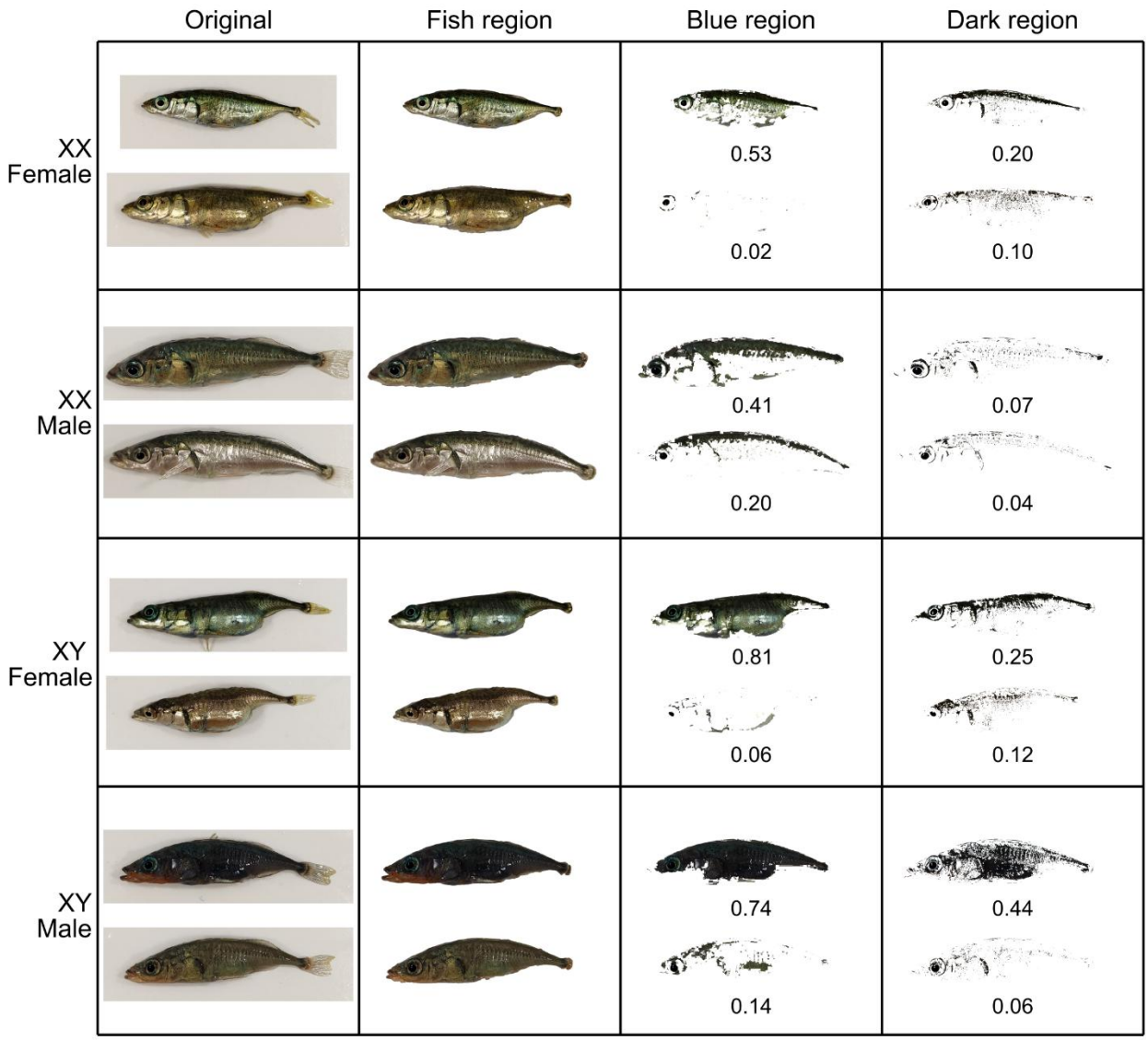

S8 Fig. Analysis of nuptial coloration in wildtype and sex reversed stickleback. Representative high and low coloration individual for XX wildtype females, XX *Tg(amhy,EGFP)* males, XY *amhy*-KO females, and XY wildtype males. Blue and darkened regions were quantified for each individual. Coloration proportion values are shown below each individual.

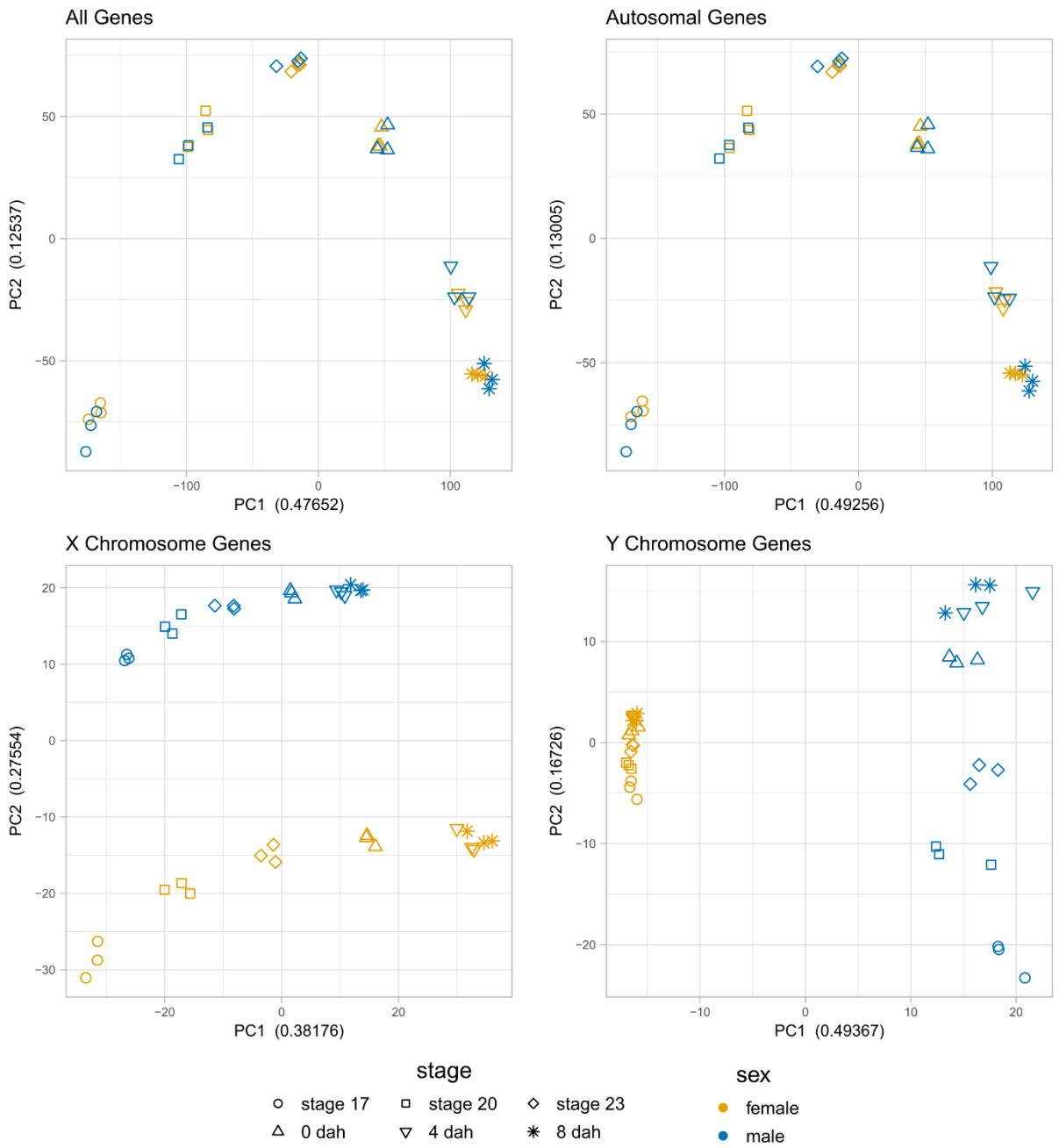

S9 Fig. PCA plots of normalized gene expression counts. Principal components 1 and 2 with the Proportion of Variance Explained on the X and Y axes, respectively. When analyzing all genes or autosomal genes only, samples group by developmental stage and not sex. X chromosome genes show separation by both stage and sex. Y chromosome genes group primarily by sex with male samples separate by developmental stage.

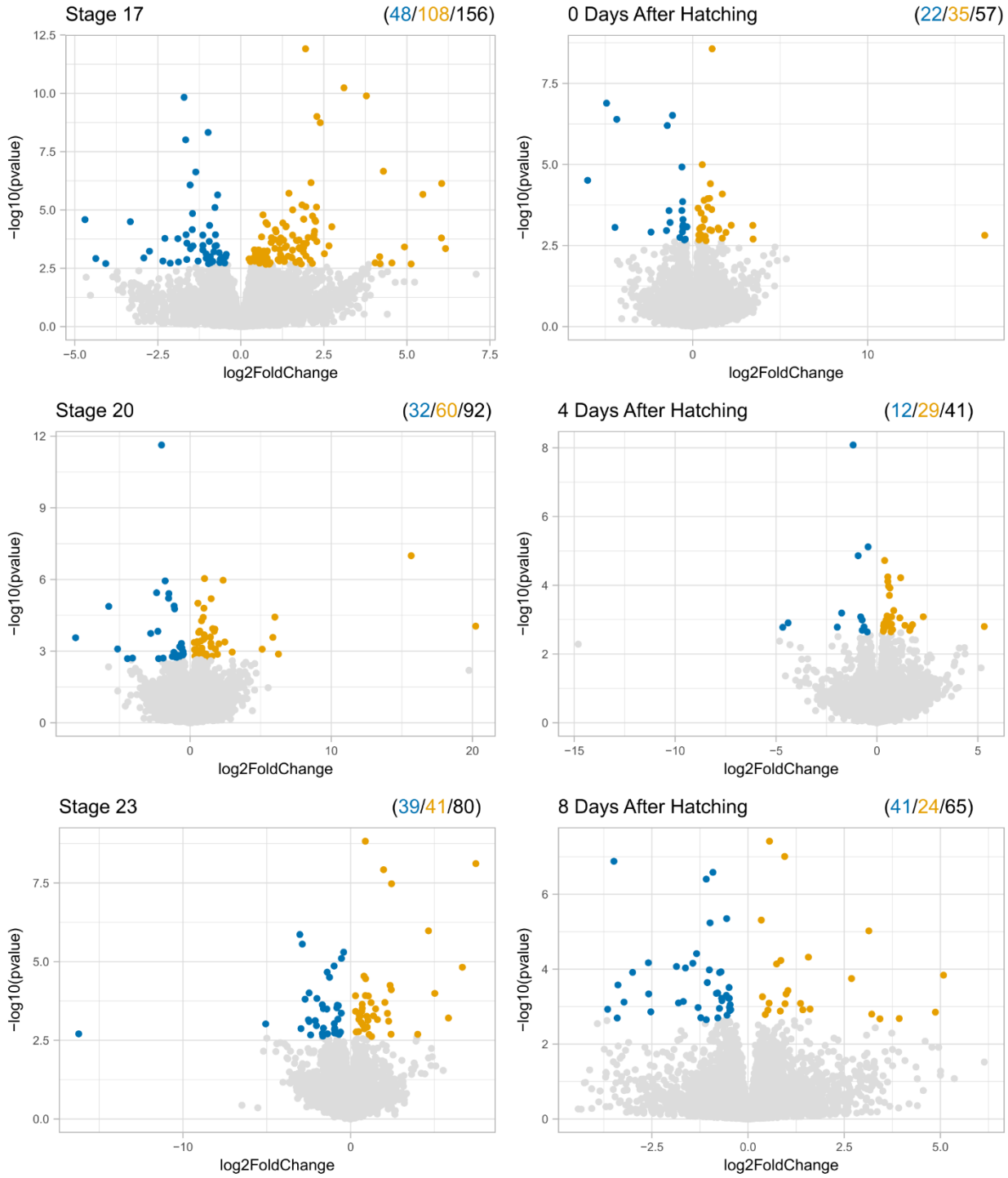

S10 Fig. Volcano plots of female to male differential expression by stage. Positive log2 Fold Change values indicate higher expression in females, and negative values indicate higher expression in males. Significant genes ($p < 0.05$) are shaded. The number of male biased, female biased, and total differentially expressed genes are shown above each plot.

957 **S1 Table. Viability and Hatching rates of crosses between wildtype XX females and**
958 **wildtype XY males.**

Female	Male	Clutch Size	Viable	Hatched	Viable:total	Hatched:total	hatched:viable
1	A	95	95	94	1.0000	0.9895	0.9895
2	A	66	65	64	0.9848	0.9697	0.9846
3	A	91	61	60	0.6703	0.6593	0.9836
4	B	110	107	107	0.9727	0.9727	1.0000
5	B	65	58	58	0.8923	0.8923	1.0000
6	B	116	116	116	1.0000	1.0000	1.0000
7	C	107	100	98	0.9346	0.9159	0.9800
8	C	90	54	43	0.6000	0.4778	0.7963
9	C	117	74	68	0.6325	0.5812	0.9189
total	A	252	221	218	0.8770	0.8651	0.9864
total	B	291	281	281	0.9656	0.9656	1.0000
total	C	314	228	209	0.7261	0.6656	0.9167
total	total	857	730	708	0.8518	0.8261	0.9699

959

960 **S2 Table. Viability and Hatching rates of crosses from F1 XY *amhy*-KO females with**
961 **wildtype XY males.**

Female	Cross number	Clutch Size	Viable	Hatched	Viable:total	Hatched:total	Hatched:viable
A	1	43	1	1	0.0233	0.0233	1.0000
B	1	51	2	0	0.0392	0.0000	0.0000
C	1	63	4	2	0.0635	0.0317	0.5000
C	2	99	24	21	0.2424	0.2121	0.8750
C	3	81	11	6	0.1358	0.0741	0.5455
C	4	100	78	54	0.7800	0.5400	0.6923
C	5	89	70	46	0.7865	0.5169	0.6571

962

963

S3 Table. Viability and Hatching rates of crosses from F2 XX or XY *amhy*-KO females a wildtype XY male.

Genotype	Clutch Size	Viable	Hatched	Viable:total	Hatched:total	Hatched:viable
XX	57	57	57	1.0000	1.0000	1.0000
XX	112	105	34	0.9375	0.3036	0.3238
XX	56	55	55	0.9821	0.9821	1.0000
XX	136	90	47	0.6618	0.3456	0.5222
XX	94	94	79	1.0000	0.8404	0.8404
XY	84	6	2	0.0714	0.0238	0.3333
XY	65	0	0	0.0000	0.0000	NA
XY	98	0	0	0.0000	0.0000	NA
XY	22	0	0	0.0000	0.0000	NA
XY	72	6	4	0.0833	0.0556	0.6667
XY	92	0	0	0.0000	0.0000	NA
Total XX	455	401	272	0.8813	0.5978	0.6783
Total XY	433	12	6	0.0277	0.0139	0.5000

S4 Table. Wald z-test statistics of estimated marginal means from beta regression of the effect genotype on nuptial coloration.

Comparison	Estimate	Standard Error	z.ratio	p.value
Blue proportion XXWT-XXTG	-0.0951	0.0593	-1.606	0.3754
Blue proportion XXWT-XYKO	-0.2144	0.0793	-2.702	**0.0348**
Blue proportion XXWT-XYWT	-0.3622	0.0738	-4.906	**<0.0001**
Blue proportion XXTG-XYKO	-0.1192	0.0718	-1.66	0.3451
Blue proportion XXTG-XYWT	-0.2671	0.0657	-4.066	**0.0003**
Blue proportion XYKO-XYWT	-0.1478	0.0843	-1.754	0.2956
Dark proportion XXWT-XXTG	0.0458	0.0197	2.322	0.093
Dark proportion XXWT-XYKO	-0.0563	0.0249	-2.26	0.1074
Dark proportion XXWT-XYWT	-0.1047	0.047	-2.226	0.1161
Dark proportion XXTG-XYKO	-0.1021	0.0266	-3.834	**0.0007**
Dark proportion XXTG-XYWT	-0.1505	0.0479	-3.138	**0.0092**
Dark proportion XYKO-XYWT	-0.0484	0.0503	-0.961	0.7716

970 **S5 Table. Sequence conservation of the threespine *amh* to threespine *amhy* and ninespine *amh*.**

Threespine *amh* and threespine *amhy*											
	Exon 1	Exon 2	Exon 3	Exon 4	Exon 5	Exon 6	Exon 7	CDS	Introns	2kb Upstream	2kb Downstream
Sequence identity	0.760	0.682	0.812	0.866	0.790	0.846	0.742	0.780	0.286	0.365	0.376
dN/dS	0.583	0.362	0.512	0.803	0.651	0.373	0.723	0.534	-	-	-
Threespine *amh* and ninespine *amh*											
	Exon 1	Exon 2	Exon 3	Exon 4	Exon 5	Exon 6	Exon 7	CDS	Introns	2kb Upstream	2kb Downstream
Sequence identity	0.791	0.769	0.890	0.920	0.870	0.905	0.936	0.879	0.668	0.595	0.660
dN/dS	0.597	0.425	1.003	0.441	0.266	0.565	0.278	0.467	-	-	-

971

S6 Table. Combined *amh* and *amhy* expression show significant differences between males and females at later stages.

stage	stage 17		stage 20		stage 23		0 dph		4 dph		8 dph	
sex	female	male	female	male	female	male	female	male	female	male	female	male
amh normalized counts	24.08	28.94	15.13	34.03	32.04	17.02	18.72	37.12	6.94	12.47	17.04	23.57
	34.14	13.17	22.49	18.61	17.94	12.90	29.62	14.87	7.01	10.98	12.34	14.82
	27.42	25.48	32.20	17.49	16.36	24.01	18.31	23.89	17.46	6.78	10.36	19.66
Mean	28.55	22.53	23.27	23.38	22.11	17.98	22.22	25.29	10.47	10.08	13.25	19.35
SD	5.12	8.29	8.56	9.24	8.64	5.62	6.41	11.19	6.06	2.95	3.43	4.38
amhy normalized counts	0.00	8.40	0.00	0.95	0.00	13.62	0.85	19.88	0.00	37.42	0.00	13.60
	0.00	10.13	0.00	4.65	0.00	8.60	0.00	20.12	0.00	20.58	0.00	33.13
	0.00	2.83	0.00	2.06	0.00	11.08	2.93	8.76	0.00	16.27	0.00	9.44
Mean	0.00	7.12	0.00	2.55	0.00	11.10	1.26	16.25	0.00	24.76	0.00	18.72
sd	0.00	3.81	0.00	1.90	0.00	2.51	1.51	6.49	0.00	11.18	0.00	12.65
length adjusted *amhy* counts	0.00	13.11	0.00	1.48	0.00	21.25	1.33	31.03	0.00	58.40	0.00	21.22
	0.00	15.81	0.00	7.26	0.00	13.42	0.00	31.40	0.00	32.11	0.00	51.70
	0.00	4.42	0.00	3.21	0.00	17.29	4.57	13.67	0.00	25.39	0.00	14.73
Mean	0.00	11.11	0.00	3.98	0.00	17.32	1.97	25.37	0.00	38.63	0.00	29.22
SD	0.00	5.95	0.00	2.97	0.00	3.91	2.35	10.13	0.00	17.44	0.00	19.74
P *amhy* ≠ 0.5**amh*	-	0.9730	-	0.0830	-	**0.0454**	-	0.1496	-	0.0783	-	0.2275
amh + length adj. *amhy* counts	24.08	42.05	15.13	35.51	32.04	38.27	20.05	68.15	6.94	70.87	17.04	44.78
	34.14	28.98	22.49	25.86	17.94	26.32	29.62	46.27	7.01	43.09	12.34	66.53
	27.42	29.89	32.20	20.71	16.36	41.31	22.88	37.56	17.46	32.16	10.36	34.39
Mean	28.55	33.64	23.27	27.36	22.11	35.30	24.19	50.66	10.47	48.71	13.25	48.57
SD	5.12	7.30	8.56	7.51	8.64	7.92	4.91	15.76	6.06	19.96	3.43	16.40
P total *amh* males > females	0.1922		0.2843		0.0618		**0.0448**		**0.0347**		**0.0297**	

Length adjusted *amhy* counts were calculated by multiplying *amhy* normalized read counts by transcript length of *amh* (3895 bp) divided by *amhy* (2496 bp). P values show two tailed Welch's t-test for a difference between *amhy* and one half *amh* expression in males at each stage and one tailed Welch's t-test for a greater total *amh* dosage in males than in females at each stage. Significant values are bolded ($p < 0.05$).

977 **S7 Table. PCR primers used in this study.**

Assay	Forward primer	Reverse primer
XY *idh* genotyping	5'-GGGACGAGCAAGATTTATT-3'	5'-TTATCGTTAGCCAGGAGATGG-3'
amhy exon 1 genotyping, *amhy* transgene detection	5'-TTGGTGGGTTGATGCTCTGC-3'	5'-CTATGTGAGAGACTGTGGCGG-3'
amhy exon 3 genotyping	5'-TCAGTTTGGAATCTGCACTGTT-3'	5'-GGATGCAGTGATTTACTGGTGA-3'
amhy 2.3 kb deletion genotyping	5'-CACAGTCCTTCGACTCCTTCG-3'	5'-GAGACCATGGTGACTGGCTC-3'
amh exon 1 genotyping	5'-GGCAGTGAGAAGGGAAGGTG-3'	5'-GGCCTCTGGTGATGGGAATG-3'
amh exon 3 genotyping	5'-CAGCCGGAGTCAGTTTGGAA-3'	5'-TCATGCATCGTCGACTGGAG-3'
EGFP transgene detection	5'-ATCATGGCCGACAAGCAGAA-3'	5'-AACTCCAGCAGGACCATGTG-3'
dmrt1 riboprobe cloning	5'-AGCAGCACCGAGAAGCAG-3'	5'-CTCGTTGACGTTGCCCATGA-3'
gsdf riboprobe cloning	5'-TTTTGTCACGGCGATGCTTC-3'	5'-AGGAAATGACGAGGGTGCTG-3'
foxl2 riboprobe cloning	5'-GAGAAGGTCCCGGAGAAAGC-3'	5'-GCAGTGCATCATCGAGAGCT-3'
cyp19a1a riboprobe cloning	5'-CCTTGTTTCTGTCTGGGCCT-3'	5'-TTGAGGAGCAGCAGCATGA-3'
Riboprobe template synthesis	5'-TAATACGACTCACTATAGGG-3'	5'-TAATACGACTCACTATAGGG-3'

978
979 **S1 File. RNA-seq summary and statistics**
980
981 **S2 File. Sequence files**
982
983 **S3 File. Coloration data**
984

References

1. Bachtrog D, Mank JE, Peichel CL, Kirkpatrick M, Otto SP, Ashman T-L, et al. Sex Determination: Why So Many Ways of Doing It? PLoS Biol. 2014;12: e1001899. doi:10.1371/journal.pbio.1001899

2. Capel B. Vertebrate sex determination: evolutionary plasticity of a fundamental switch. Nat Rev Genet. 2017;18: 675–689. doi:10.1038/nrg.2017.60

3. Weber C, Capel B. Sex determination without sex chromosomes. Philosophical Transactions of the Royal Society B: Biological Sciences. 2021;376: 20200109. doi:10.1098/rstb.2020.0109

4. Charlesworth D, Charlesworth B, Marais G. Steps in the evolution of heteromorphic sex chromosomes. Heredity. 2005;95: 118–128. doi:10.1038/sj.hdy.6800697

5. Charlesworth B, Charlesworth D. A Model for the Evolution of Dioecy and Gynodioecy. The American Naturalist. 1978;112: 975–997. doi:10.1086/283342

6. Ponnikas S, Sigeman H, Abbott JK, Hansson B. Why Do Sex Chromosomes Stop Recombining? Trends in Genetics. 2018;34: 492–503. doi:10.1016/j.tig.2018.04.001

7. Pan Q, Kay T, Depincé A, Adolfi M, Schartl M, Guiguen Y, et al. Evolution of master sex determiners: TGF-β signalling pathways at regulatory crossroads. Philosophical Transactions of the Royal Society B: Biological Sciences. 2021;376: 20200091. doi:10.1098/rstb.2020.0091

8. Takehana Y, Matsuda M, Myosho T, Suster ML, Kawakami K, Shin-I T, et al. Co-option of Sox3 as the male-determining factor on the Y chromosome in the fish Oryzias dancena. Nat Commun. 2014;5: 4157. doi:10.1038/ncomms5157

9. Shan Z, Nanda I, Wang Y, Schmid M, Vortkamp A, Haaf T. Sex-specific expression of an evolutionarily conserved male regulatory gene, DMRT1, in birds. Cytogenetics and Cell Genetics. 2000;89: 252–257. doi:10.1159/000015626

10. Yoshimoto S, Okada E, Umemoto H, Tamura K, Uno Y, Nishida-Umehara C, et al. A W-linked DM-domain gene, DM-W, participates in primary ovary development in Xenopus laevis. Proceedings of the National Academy of Sciences. 2008;105: 2469–2474. doi:10.1073/pnas.0712244105

11. Matsuda M, Nagahama Y, Shinomiya A, Sato T, Matsuda C, Kobayashi T, et al. DMY is a Y-specific DM-domain gene required for male development in the medaka fish. Nature. 2002;417: 559–563. doi:10.1038/nature751

12. Nanda I, Kondo M, Hornung U, Asakawa S, Winkler C, Shimizu A, et al. A duplicated copy of DMRT1 in the sex-determining region of the Y chromosome of the medaka, Oryzias latipes. Proceedings of the National Academy of Sciences. 2002;99: 11778–11783. doi:10.1073/pnas.182314699

1021 13. Hattori RS, Murai Y, Oura M, Masuda S, Majhi SK, Sakamoto T, et al. A Y-linked anti-
1022 Mullerian hormone duplication takes over a critical role in sex determination. Proceedings
1023 of the National Academy of Sciences. 2012;109: 2955–2959.
1024 doi:10.1073/pnas.1018392109

1025 14. Hattori RS, Somoza GM, Fernandino JI, Colautti DC, Miyoshi K, Gong Z, et al. The
1026 Duplicated Y-specific amhy Gene Is Conserved and Linked to Maleness in Silversides of
1027 the Genus Odontesthes. Genes. 2019;10: 679. doi:10.3390/genes10090679

1028 15. Hattori RS, Kumazawa K, Nakamoto M, Nakano Y, Yamaguchi T, Kitano T, et al. Y-specific
1029 amh allele, amhy, is the master sex-determining gene in Japanese flounder Paralichthys
1030 olivaceus. Frontiers in Genetics. 2022;13. Available:
1031 https://www.frontiersin.org/articles/10.3389/fgene.2022.1007548

1032 16. Li M, Sun Y, Zhao J, Shi H, Zeng S, Ye K, et al. A Tandem Duplicate of Anti-Müllerian
1033 Hormone with a Missense SNP on the Y Chromosome Is Essential for Male Sex
1034 Determination in Nile Tilapia, Oreochromis niloticus. Naruse K, editor. PLoS Genet.
1035 2015;11: e1005678. doi:10.1371/journal.pgen.1005678

1036 17. Rondeau EB, Laurie CV, Johnson SC, Koop BF. A PCR assay detects a male-specific
1037 duplicated copy of Anti-Müllerian hormone (amh) in the lingcod (Ophiodon elongatus).
1038 BMC Research Notes. 2016;9: 230. doi:10.1186/s13104-016-2030-6

1039 18. Bej DK, Miyoshi K, Hattori RS, Strüssmann CA, Yamamoto Y. A Duplicated, Truncated
1040 amh Gene Is Involved in Male Sex Determination in an Old World Silverside. G3
1041 Genes|Genomes|Genetics. 2017;7: 2489–2495. doi:10.1534/g3.117.042697

1042 19. Pan Q, Feron R, Yano A, Guyomard R, Jouanno E, Vigouroux E, et al. Identification of the
1043 master sex determining gene in Northern pike (Esox lucius) reveals restricted sex
1044 chromosome differentiation. PLOS Genetics. 2019;15: e1008013.
1045 doi:10.1371/journal.pgen.1008013

1046 20. Peichel CL, McCann SR, Ross JA, Naftaly AFS, Urton JR, Cech JN, et al. Assembly of
1047 the threespine stickleback Y chromosome reveals convergent signatures of sex
1048 chromosome evolution. Genome Biol. 2020;21: 177. doi:10.1186/s13059-020-02097-x

1049 21. Song W, Xie Y, Sun M, Li X, Fitzpatrick CK, Vaux F, et al. A duplicated amh is the master
1050 sex-determining gene for Sebastes rockfish in the Northwest Pacific. Open Biology.
1051 2021;11: 210063. doi:10.1098/rsob.210063

1052 22. Jeffries DL, Mee JA, Peichel CL. Identification of a candidate sex determination gene in
1053 Culaea inconstans suggests convergent recruitment of an Amh duplicate in two lineages
1054 of stickleback. Journal of Evolutionary Biology. 2022;n/a. doi:10.1111/jeb.14034

1055 23. Zhao H, Li J, Xiao Z, Xiao Y. Dose-dependent role of AMH and AMHR2 signaling in male
1056 differentiation and regulation of sex determination in Spotted knifejaw (Oplegnathus
1057 punctatus) with X1X1X2X2/X1X2Y chromosome system. Cell Communication and
1058 Signaling. 2025;23: 59. doi:10.1186/s12964-025-02038-w

1059 24. Wang T, Gong G, Li Z, Niu J-S, Du W-X, Wang Z-W, et al. Genomic Anatomy of
1060 Homozygous XX Females and YY Males Reveals Early Evolutionary Trajectory of Sex-

determining Gene and Sex Chromosomes in Silurus Fishes. Molecular Biology and Evolution. 2024;41: msae169. doi:10.1093/molbev/msae169

25. Cortez D, Marin R, Toledo-Flores D, Froidevaux L, Liechti A, Waters PD, et al. Origins and functional evolution of Y chromosomes across mammals. Nature. 2014;508: 488–493. doi:10.1038/nature13151

26. Mullen RD, Ontiveros AE, Moses MM, Behringer RR. AMH and AMHR2 mutations: A spectrum of reproductive phenotypes across vertebrate species. Developmental Biology. 2019;455: 1–9. doi:10.1016/j.ydbio.2019.07.006

27. Howard JA, Hart KN, Thompson TB. Molecular Mechanisms of AMH Signaling. Frontiers in Endocrinology. 2022;13. Available: https://www.frontiersin.org/articles/10.3389/fendo.2022.927824

28. Baarends WM, Helmond MJL van, Post M, Schoot PJCM van der, Hoogerbrugge JW, Winter JP de, et al. A novel member of the transmembrane serine/threonine kinase receptor family is specifically expressed in the gonads and in mesenchymal cells adjacent to the müllerian duct. Development. 1994;120: 189–197. doi:10.1242/dev.120.1.189

29. Josso N, di Clemente N, Gouédard L. Anti-Müllerian hormone and its receptors. Molecular and Cellular Endocrinology. 2001;179: 25–32. doi:10.1016/S0303-7207(01)00467-1

30. Mishina Y, Whitworth DJ, Racine C, Behringer RR. High Specificity of Müllerian-Inhibiting Substance Signaling in Vivo*. Endocrinology. 1999;140: 2084–2088. doi:10.1210/endo.140.5.6705

31. Jost A. The Age Factor in the Castration of Male Rabbit Fetuses. Proceedings of the Society for Experimental Biology and Medicine. 1947;66: 302–303. doi:10.3181/00379727-66-16071

32. Morinaga C, Saito D, Nakamura S, Sasaki T, Asakawa S, Shimizu N, et al. The hotei mutation of medaka in the anti-Müllerian hormone receptor causes the dysregulation of germ cell and sexual development. PNAS. 2007;104: 9691–9696. doi:10.1073/pnas.0611379104

33. Pfennig F, Standke A, Gutzeit HO. The role of Amh signaling in teleost fish – Multiple functions not restricted to the gonads. General and Comparative Endocrinology. 2015;223: 87–107. doi:10.1016/j.ygcen.2015.09.025

34. Yan Y-L, Batzel P, Titus T, Sydes J, Desvignes T, BreMiller R, et al. A Hormone That Lost Its Receptor: Anti-Müllerian Hormone (AMH) in Zebrafish Gonad Development and Sex Determination. Genetics. 2019;213: 529–553. doi:10.1534/genetics.119.302365

35. Ross JA, Urton JR, Boland J, Shapiro MD, Peichel CL. Turnover of Sex Chromosomes in the Stickleback Fishes (Gasterosteidae). PLOS Genetics. 2009;5: e1000391. doi:10.1371/journal.pgen.1000391

36. Dixon G, Kitano J, Kirkpatrick M. The Origin of a New Sex Chromosome by Introgression between Two Stickleback Fishes. Molecular Biology and Evolution. 2019;36: 28–38. doi:10.1093/molbev/msy181

37. Natri HM, Merilä J, Shikano T. The evolution of sex determination associated with a chromosomal inversion. Nat Commun. 2019;10: 145. doi:10.1038/s41467-018-08014-y

38. Sardell JM, Josephson MP, Dalziel AC, Peichel CL, Kirkpatrick M. Heterogeneous Histories of Recombination Suppression on Stickleback Sex Chromosomes. Molecular Biology and Evolution. 2021;38: 4403–4418. doi:10.1093/molbev/msab179

39. Peichel CL, Ross JA, Matson CK, Dickson M, Grimwood J, Schmutz J, et al. The Master Sex-Determination Locus in Threespine Sticklebacks Is on a Nascent Y Chromosome. Current Biology. 2004;14: 1416–1424. doi:10.1016/j.cub.2004.08.030

40. Pigott GC, Akel MA, Rogers MGQ, Flanagan ME, Marlette EG, Treaster MJ, et al. Evidence for Variation in the Genetic Basis of Sex Determination in Brook Stickleback (Culaea inconstans). Ecology and Evolution. 2025;15: e70955. doi:10.1002/ece3.70955

41. Erickson PA, Ellis NA, Miller CT. Microinjection for Transgenesis and Genome Editing in Threespine Sticklebacks. J Vis Exp. 2016 [cited 30 Jan 2021]. doi:10.3791/54055

42. Nath S, Shaw DE, White MA. Improved contiguity of the threespine stickleback genome using long-read sequencing. G3 Genes|Genomes|Genetics. 2021;11. doi:10.1093/g3journal/jkab007

43. Aguirre WE, Ellis KE, Kusenda M, Bell MA. Phenotypic variation and sexual dimorphism in anadromous threespine stickleback: implications for postglacial adaptive radiation. Biological Journal of the Linnean Society. 2008;95: 465–478. doi:10.1111/j.1095-8312.2008.01075.x

44. Leinonen T, Cano JM, Merilä J. Genetic basis of sexual dimorphism in the threespine stickleback Gasterosteus aculeatus. Heredity. 2011;106: 218–227. doi:10.1038/hdy.2010.104

45. Kitano J, Mori S, Peichel CL. Sexual Dimorphism in the External Morphology of the Threespine Stickleback (Gasterosteus Aculeatus). Copeia. 2007;2007: 336–349. doi:10.1643/0045-8511(2007)7%5B336:SDITEM%5D2.0.CO;2

46. Aguirre WE, Akinpelu O. Sexual dimorphism of head morphology in three-spined stickleback Gasterosteus aculeatus. Journal of Fish Biology. 2010;77: 802–821. doi:10.1111/j.1095-8649.2010.02705.x

47. Toli EA, Noreikiene K, DeFaveri J, Merilä J. Environmental enrichment, sexual dimorphism, and brain size in sticklebacks. Ecology and Evolution. 2017;7: 1691–1698. doi:10.1002/ece3.2717

48. Kotrschal A, Räsänen K, Kristjánsson BK, Senn M, Kolm N. Extreme Sexual Brain Size Dimorphism in Sticklebacks: A Consequence of the Cognitive Challenges of Sex and Parenting? PLOS ONE. 2012;7: e30055. doi:10.1371/journal.pone.0030055

49. McGee MD, Wainwright PC. Sexual dimorphism in the feeding mechanism of threespine stickleback. Journal of Experimental Biology. 2013;216: 835–840. doi:10.1242/jeb.074948

50. Whoriskey FG, FitzGerald GJ. Sex, cannibalism and sticklebacks. Behav Ecol Sociobiol. 1985;18: 15–18. doi:10.1007/BF00299233

51. King AJ, Fürtbauer I, Mamuneas D, James C, Manica A. Sex-Differences and Temporal Consistency in Stickleback Fish Boldness. PLOS ONE. 2013;8: e81116. doi:10.1371/journal.pone.0081116

52. FitzGerald GJ. The Reproductive Behavior of the Stickleback. Scientific American. 1993;268: 80–85.

53. Bell MA, Foster SA. The Evolutionary Biology of the Threespine Stickleback. The Journal of Animal Ecology. 1994;64: 418. doi:10.2307/5902

54. Pressley PH. Parental Effort and the Evolution of Nest-Guarding Tactics in the Threespine Stickleback, Gasterosteus aculeatus L. Evolution. 1981;35: 282–295. doi:10.2307/2407838

55. Bakker TCM, Künzler R, Mazzi D. Condition-related mate choice in sticklebacks. Nature. 1999;401: 234–234. doi:10.1038/45727

56. Milinski M, Bakker TCM. Female sticklebacks use male coloration in mate choice and hence avoid parasitized males. Nature. 1990;344: 330–333. doi:10.1038/344330a0

57. Conte GL, Schluter D. Experimental Confirmation That Body Size Determines Mate Preference via Phenotype Matching in a Stickleback Species Pair. Evolution. 2013;67: 1477–1484. doi:10.1111/evo.12041

58. Andreou D, Eizaguirre C, Boehm T, Milinski M. Mate choice in sticklebacks reveals that immunogenes can drive ecological speciation. Behavioral Ecology. 2017;28: 953–961. doi:10.1093/beheco/arx074

59. Milinski M. The function of mate choice in sticklebacks: optimizing Mhc genetics. Journal of Fish Biology. 2003;63: 1–16. doi:10.1111/j.1095-8649.2003.00215.x

60. Flamarique IN, Bergstrom C, Cheng CL, Reimchen TE. Role of the iridescent eye in stickleback female mate choice. Journal of Experimental Biology. 2013;216: 2806–2812. doi:10.1242/jeb.084889

61. Barker TCM, Milinski M. The advantages of being red: Sexual selection in the stickleback. Marine & Freshwater Behaviour & Phy. 1993 [cited 21 Apr 2025]. doi:10.1080/10236249309378870

62. Candolin U. Reproduction under predation risk and the trade–off between current and future reproduction in the threespine stickleback. Proceedings of the Royal Society of London Series B: Biological Sciences. 1998;265: 1171–1175. doi:10.1098/rspb.1998.0415

1172 63. Johnson S, Candolin U. Predation cost of a sexual signal in the threespine stickleback.
1173 Behavioral Ecology. 2017;28: 1160–1165. doi:10.1093/beheco/arx080

1174 64. Borg B, Mayer I, Hoffmann E, Österman A. 11-ketotestosterone is not responsible for the
1175 entire testicular effect on male reproductive behaviour in the threespine stickleback.
1176 Behav. 2008;145: 509–525. doi:10.1163/156853908792451548

1177 65. Shibata Y, Paul-Prasanth B, Suzuki A, Usami T, Nakamoto M, Matsuda M, et al.
1178 Expression of gonadal soma derived factor (GSDF) is spatially and temporally correlated
1179 with early testicular differentiation in medaka. Gene Expression Patterns. 2010;10: 283–
1180 289. doi:10.1016/j.gep.2010.06.005

1181 66. Guo Y, Cheng H, Huang X, Gao S, Yu H, Zhou R. Gene structure, multiple alternative
1182 splicing, and expression in gonads of zebrafish *Dmrt1*. Biochemical and Biophysical
1183 Research Communications. 2005;330: 950–957. doi:10.1016/j.bbrc.2005.03.066

1184 67. von Hofsten J, Larsson A, Olsson P e. Novel steroidogenic factor-1 homolog (ff1d) is
1185 coexpressed with anti-Mullerian hormone (AMH) in zebrafish. Developmental Dynamics.
1186 2005;233: 595–604. doi:10.1002/dvdy.20335

1187 68. Johnsen H, Seppola M, Torgersen JS, Delghandi M, Andersen Ø. Sexually dimorphic
1188 expression of *dmrt1* in immature and mature Atlantic cod (*Gadus morhua* L.).
1189 Comparative Biochemistry and Physiology Part B: Biochemistry and Molecular Biology.
1190 2010;156: 197–205. doi:10.1016/j.cbpb.2010.03.009

1191 69. von Schalburg KR, Gowen BE, Rondeau EB, Johnson NW, Minkley DR, Leong JS, et al.
1192 Sex-specific expression, synthesis and localization of aromatase regulators in one-year-
1193 old Atlantic salmon ovaries and testes. Comparative Biochemistry and Physiology Part B:
1194 Biochemistry and Molecular Biology. 2013;164: 236–246. doi:10.1016/j.cbpb.2013.01.004

1195 70. Kossack ME, Draper BW. Genetic regulation of sex determination and maintenance in
1196 zebrafish (Danio rerio). Curr Top Dev Biol. 2019;134: 119–149.
1197 doi:10.1016/bs.ctdb.2019.02.004

1198 71. Urasaki A, Morvan G, Kawakami K. Functional Dissection of the Tol2 Transposable
1199 Element Identified the Minimal cis-Sequence and a Highly Repetitive Sequence in the
1200 Subterminal Region Essential for Transposition. Genetics. 2006;174: 639–649.
1201 doi:10.1534/genetics.106.060244

1202 72. Kawakami K, Takeda H, Kawakami N, Kobayashi M, Matsuda N, Mishina M. A
1203 Transposon-Mediated Gene Trap Approach Identifies Developmentally Regulated Genes
1204 in Zebrafish. Developmental Cell. 2004;7: 133–144. doi:10.1016/j.devcel.2004.06.005

1205 73. Kim JH, Lee S-R, Li L-H, Park H-J, Park J-H, Lee KY, et al. High Cleavage Efficiency of a
1206 2A Peptide Derived from Porcine Teschovirus-1 in Human Cell Lines, Zebrafish and Mice.
1207 PLOS ONE. 2011;6: e18556. doi:10.1371/journal.pone.0018556

1208 74. Liu Z, Chen O, Wall JBJ, Zheng M, Zhou Y, Wang L, et al. Systematic comparison of 2A
1209 peptides for cloning multi-genes in a polycistronic vector. Scientific Reports. 2017;7:
1210 2193. doi:10.1038/s41598-017-02460-2

1211 75. Mosimann C, Kaufman CK, Li P, Pugach EK, Tamplin OJ, Zon LI. Ubiquitous transgene
1212 expression and Cre-based recombination driven by the ubiquitin promoter in zebrafish.
1213 Development. 2011;138: 169–177. doi:10.1242/dev.059345

1214 76. Ueda Y, Mizuno N, Araki M. Transgenic Xenopus laevis with the ef1-α promoter as an
1215 experimental tool for amphibian retinal regeneration study. genesis. 2012;50: 642–650.
1216 doi:10.1002/dvg.22024

1217 77. Behringer RR, Cate RL, Froelick GJ, Palmiter RD, Brinster RL. Abnormal sexual
1218 development in transgenic mice chronically expressing Müllerian inhibiting substance.
1219 Nature. 1990;345: 167–170. doi:10.1038/345167a0

1220 78. Lambeth LS, Morris K, Ayers KL, Wise TG, O'Neil T, Wilson S, et al. Overexpression of
1221 Anti-Müllerian Hormone Disrupts Gonadal Sex Differentiation, Blocks Sex Hormone
1222 Synthesis, and Supports Cell Autonomous Sex Development in the Chicken.
1223 Endocrinology. 2016;157: 1258–1275. doi:10.1210/en.2015-1571

1224 79. Square TA, Mackey EJ, Sundaram S, Weksler NC, Chen ZZ, Narayanan SN, et al.
1225 Modulation of tooth regeneration through opposing responses to Wnt and BMP signals in
1226 teleosts. Development. 2023;150: dev202168. doi:10.1242/dev.202168

1227 80. Lu S, Cullen BR. Analysis of the stimulatory effect of splicing on mRNA production and
1228 utilization in mammalian cells. RNA. 2003;9: 618–630. doi:10.1261/rna.5260303

1229 81. Nott A, Meislin SH, Moore MJ. A quantitative analysis of intron effects on mammalian
1230 gene expression. RNA. 2003;9: 607–617. doi:10.1261/rna.5250403

1231 82. Wootton RJ. A Functional Biology of Sticklebacks. 1st ed. University of California Press;
1232 1984. doi:10.2307/jj.8306147

1233 83. Varadharajan S, Rastas P, Löytynoja A, Matschiner M, Calboli FCF, Guo B, et al. A High-
1234 Quality Assembly of the Nine-Spined Stickleback (Pungitius pungitius) Genome. Genome
1235 Biology and Evolution. 2019;11: 3291–3308. doi:10.1093/gbe/evz240

1236 84. Bachtrog D. Y-chromosome evolution: emerging insights into processes of Y-chromosome
1237 degeneration. Nat Rev Genet. 2013;14: 113–124. doi:10.1038/nrg3366

1238 85. Swarup H. Stages in the Development of the Stickleback Gasterosteus aculeatus (L.).
1239 Development. 1958;6: 373–383.

1240 86. Lewis ZR, McClellan MC, Postlethwait JH, Cresko WA, Kaplan RH. Female-specific
1241 increase in primordial germ cells marks sex differentiation in threespine stickleback (
1242 *Gasterosteus aculeatus*). J Morphol. 2008;269: 909–921. doi:10.1002/jmor.10608

1243 87. Shi D-L. Interplay of RNA-binding proteins controls germ cell development in zebrafish.
1244 Journal of Genetics and Genomics. 2024;51: 889–899. doi:10.1016/j.jgg.2024.06.020

1245 88. Planells B, Gómez-Redondo I, Pericuesta E, Lonergan P, Gutiérrez-Adán A. Differential
1246 isoform expression and alternative splicing in sex determination in mice. BMC Genomics.
1247 2019;20: 202. doi:10.1186/s12864-019-5572-x

1248 89. Mindnich R, Deluca D, Adamski J. Identification and characterization of 17β-
1249 hydroxysteroid dehydrogenases in the zebrafish, *Danio rerio*. Molecular and Cellular
1250 Endocrinology. 2004;215: 19–30. doi:10.1016/j.mce.2003.11.010

1251 90. Koyama T, Nakamoto M, Morishima K, Yamashita R, Yamashita T, Sasaki K, et al. A SNP
1252 in a Steroidogenic Enzyme Is Associated with Phenotypic Sex in Seriola Fishes. Current
1253 Biology. 2019;29: 1901-1909.e8. doi:10.1016/j.cub.2019.04.069

1254 91. Lasalle A, Benech-Correa G, Brunet FG, Vizziano-Cantonnet D. hsd17b1 is a key gene
1255 for ovarian differentiation of the Siberian sturgeon. Molecular Reproduction and
1256 Development. 2024;91: e23729. doi:10.1002/mrd.23729

1257 92. Desaulniers AT, Cederberg RA, Lents CA, White BR. Expression and Role of
1258 Gonadotropin-Releasing Hormone 2 and Its Receptor in Mammals. Front Endocrinol.
1259 2017;8. doi:10.3389/fendo.2017.00269

1260 93. Sarraj MA, Sarraj ,Mai A., Chua ,Hui Kheng, Sarraj ,Mai A., Chua ,Hui Kheng, Umbers
1261 ,Alexandra, et al. Differential expression of TGFBR3 (betaglycan) in mouse ovary and
1262 testis during gonadogenesis. Growth Factors. 2007;25: 334–345.
1263 doi:10.1080/08977190701833619

1264 94. Wickramasinghe D, Becker S, Ernst MK, Resnick JL, Centanni JM, Tessarollo L, et al.
1265 Two CDC25 homologues are differentially expressed during mouse development.
1266 Development. 1995;121: 2047–2056. doi:10.1242/dev.121.7.2047

1267 95. Namgoong S, Kim N-H. Meiotic spindle formation in mammalian oocytes: implications for
1268 human infertility†. Biology of Reproduction. 2018;98: 153–161. doi:10.1093/biolre/iox145

1269 96. Strüssmann CA, Saito T, Usui M, Yamada H, Takashima F. Thermal thresholds and critical
1270 period of thermolabile sex determination in two atherinid fishes, Odontesthes bonariensis
1271 and Patagonina hatcheri. Journal of Experimental Zoology. 1997;278: 167–177.
1272 doi:10.1002/(SICI)1097-010X(19970615)278:3%3C167::AID-JEZ6%3E3.0.CO;2-M

1273 97. Baroiller JF, D'Cotta H, Bezault E, Wessels S, Hoerstgen-Schwark G. Tilapia sex
1274 determination: Where temperature and genetics meet. Comparative Biochemistry and
1275 Physiology Part A: Molecular & Integrative Physiology. 2009;153: 30–38.
1276 doi:10.1016/j.cbpa.2008.11.018

1277 98. Sun P, You F, Ma D, Li J, Zhang P. Sex steroid changes during temperature-induced
1278 gonadal differentiation in (Temminck & Schegel, 1846). Journal of Applied Ichthyology.
1279 2013;29: 886–890. doi:10.1111/jai.12128

1280 99. Borg B, van den Hurk R. Oocytes in the Testes of the Three-Spined Stickleback,
1281 Gasterosteus aculeatus. Copeia. 1983;1983: 259–261. doi:10.2307/1444727

1282 100. Gercken J, Sordyl H. Intersex in feral marine and freshwater fish from northeastern
1283 Germany. Marine Environmental Research. 2002;54: 651–655. doi:10.1016/S0141-
1284 1136(02)00156-3

1285 101. Aharon D, Marlow FL. Sexual determination in zebrafish. Cell Mol Life Sci. 2021;79: 8.
1286 doi:10.1007/s00018-021-04066-4

102. Slanchev K, Stebler J, de la Cueva-Méndez G, Raz E. Development without germ cells: The role of the germ line in zebrafish sex differentiation. Proceedings of the National Academy of Sciences. 2005;102: 4074–4079. doi:10.1073/pnas.0407475102

103. Tzung K-W, Goto R, Saju JM, Sreenivasan R, Saito T, Arai K, et al. Early Depletion of Primordial Germ Cells in Zebrafish Promotes Testis Formation. Stem Cell Reports. 2015;4: 61–73. doi:10.1016/j.stemcr.2014.10.011

104. Schartl M. A comparative view on sex determination in medaka. Mechanisms of Development. 2004;121: 639–645. doi:10.1016/j.mod.2004.03.001

105. Kurokawa H, Saito D, Nakamura S, Katoh-Fukui Y, Ohta K, Baba T, et al. Germ cells are essential for sexual dimorphism in the medaka gonad. Proceedings of the National Academy of Sciences. 2007;104: 16958–16963. doi:10.1073/pnas.0609932104

106. Nakamura S, Watakabe I, Nishimura T, Picard J-Y, Toyoda A, Taniguchi Y, et al. Hyperproliferation of mitotically active germ cells due to defective anti-Müllerian hormone signaling mediates sex reversal in medaka. Development. 2012;139: 2283–2287. doi:10.1242/dev.076307

107. Tezak B, Straková B, Fullard DJ, Dupont S, McKey J, Weber C, et al. Higher temperatures directly increase germ cell number, promoting feminization of red-eared slider turtles. Current Biology. 2023;0. doi:10.1016/j.cub.2023.06.008

108. Guigon CJ, Coudouel N, Mazaud-Guittot S, Forest MG, Magre S. Follicular Cells Acquire Sertoli Cell Characteristics after Oocyte Loss. Endocrinology. 2005;146: 2992–3004. doi:10.1210/en.2005-0045

109. Lyet L, Louis F, Forest MG, Josso N, Behringer RR, Vigier B. Ontogeny of Reproductive Abnormalities Induced by Deregulation of Anti-Müllerian Hormone Expression in Transgenic Mice. Biology of Reproduction. 1995;52: 444–454. doi:10.1095/biolreprod52.2.444

110. Durlinger ALL, Kramer P, Karels B, de Jong FH, Uilenbroek JThJ, Grootegoed JA, et al. Control of Primordial Follicle Recruitment by Anti-Müllerian Hormone in the Mouse Ovary1. Endocrinology. 1999;140: 5789–5796. doi:10.1210/endo.140.12.7204

111. Lambeth LS, Ayers K, Cutting AD, Doran TJ, Sinclair AH, Smith CA. Anti-Müllerian Hormone Is Required for Chicken Embryonic Urogenital System Growth but Not Sexual Differentiation1. Biology of Reproduction. 2015;93. doi:10.1095/biolreprod.115.131664

112. Rehman Z ur, Worku T, Davis JS, Talpur HS, Bhattarai D, Kadariya I, et al. Role and mechanism of AMH in the regulation of Sertoli cells in mice. The Journal of Steroid Biochemistry and Molecular Biology. 2017;174: 133–140. doi:10.1016/j.jsbmb.2017.08.011

113. Rodriguez KF, Brown PR, Amato CM, Nicol B, Liu C-F, Xu X, et al. Somatic cell fate maintenance in mouse fetal testes via autocrine/paracrine action of AMH and activin B. Nat Commun. 2022;13: 4130. doi:10.1038/s41467-022-31486-y

114. Guiguen Y, Fostier A, Piferrer F, Chang C-F. Ovarian aromatase and estrogens: A pivotal role for gonadal sex differentiation and sex change in fish. General and Comparative Endocrinology. 2010;165: 352–366. doi:10.1016/j.ygcen.2009.03.002

115. Li M, Sun L, Wang D. Roles of estrogens in fish sexual plasticity and sex differentiation. General and Comparative Endocrinology. 2019;277: 9–16. doi:10.1016/j.ygcen.2018.11.015

116. Liu X, Dai S, Wu J, Wei X, Zhou X, Chen M, et al. Roles of anti-Müllerian hormone and its duplicates in sex determination and germ cell proliferation of Nile tilapia. Genetics. 2021; iyab237. doi:10.1093/genetics/iyab237

117. Wu K, Yue Y, Zhou L, Zhang Z, Shan H, He H, et al. Disrupting Amh and androgen signaling reveals their distinct roles in zebrafish gonadal differentiation and gametogenesis. Commun Biol. 2025;8: 1–15. doi:10.1038/s42003-025-07719-3

118. Zhang Z, Wu K, Ren Z, Ge W. Genetic evidence for Amh modulation of gonadotropin actions to control gonadal homeostasis and gametogenesis in zebrafish and its noncanonical signaling through Bmpr2a receptor. Development. 2020;147: dev189811. doi:10.1242/dev.189811

119. Ijiri S, Kaneko H, Kobayashi T, Wang D-S, Sakai F, Paul-Prasanth B, et al. Sexual Dimorphic Expression of Genes in Gonads During Early Differentiation of a Teleost Fish, the Nile Tilapia Oreochromis niloticus1. Biology of Reproduction. 2008;78: 333–341. doi:10.1095/biolreprod.107.064246

120. Czerwinski M, Natarajan A, Barske L, Looger LL, Capel B. A timecourse analysis of systemic and gonadal effects of temperature on sexual development of the red-eared slider turtle Trachemys scripta elegans. Developmental Biology. 2016;420: 166–177. doi:10.1016/j.ydbio.2016.09.018

121. Sánchez-Baizán N, Jarne-Sanz I, Roco ÁS, Schartl M, Piferrer F. Extraordinary variability in gene activation and repression programs during gonadal sex differentiation across vertebrates. Front Cell Dev Biol. 2024;12. doi:10.3389/fcell.2024.1328365

122. Kaitetzidou E, Gilfillan GD, Antonopoulou E, Sarropoulou E. Sex-biased dynamics of three-spined stickleback (Gasterosteus aculeatus) gene expression patterns. Genomics. 2022;114: 266–277. doi:10.1016/j.ygeno.2021.12.010

123. Liu X, Xiao H, Jie M, Dai S, Wu X, Li M, et al. Amh regulate female folliculogenesis and fertility in a dose-dependent manner through Amhr2 in Nile tilapia. Molecular and Cellular Endocrinology. 2020;499: 110593. doi:10.1016/j.mce.2019.110593

124. Hacker A, Capel B, Goodfellow P, Lovell-Badge R. Expression of Sry, the mouse sex determining gene. Development. 1995;121: 1603–1614. doi:10.1242/dev.121.6.1603

125. Kobayashi T, Nagahama Y. Molecular Aspects of Gonadal Differentiation in a Teleost Fish, the Nile Tilapia. Sexual Development. 2009;3: 108–117. doi:10.1159/000223076

126. Eshel O, Shirak A, Weller JI, Hulata G, Ron M. Linkage and Physical Mapping of Sex Region on LG23 of Nile Tilapia (Oreochromis niloticus). G3 Genes|Genomes|Genetics. 2012;2: 35–42. doi:10.1534/g3.111.001545

127. Liu X, Zhou L, Li W, Zhang L, Li M, Wang D. Production of fertile YY pseudofemales in Nile tilapia with LG23 as the sex chromosome. Aquaculture. 2024;587: 740870. doi:10.1016/j.aquaculture.2024.740870

128. Yamazaki W, Tan SL, Taketo T. Role of the X and Y Chromosomes in the Female Germ Cell Line Development in the Mouse (Mus musculus). Sexual Development. 2023;16: 355–364. doi:10.1159/000521151

129. Lam TJ, Nagahama Y, Chan K, Hoar WS. Overripe eggs and postovulatory corpora lutea in the threespine stickleback, Gasterosteus aculeatus L., form trachurus. Can J Zool. 1978;56: 2029–2036. doi:10.1139/z78-273

130. Roufidou C, Sebire M, Katsiadaki I, Mustafa A, Schmitz M, Mayer I, et al. Overripening of eggs and changes in reproductive hormones in the threespine stickleback, Gasterosteus aculeatus. Evol Ecol Res. 2016;17: 583–601.

131. Roufidou C, Borg B. Ovarian fluid in the three-spined stickleback : effects of egg overripening and sex steroid treatment. Journal of Fish Biology. 2019;94: 446–457. doi:10.1111/jfb.13915

132. Levy ER, Burgoyne PS. The fate of XO germ cells in the testes of XO/XY and XO/XY/XYY mouse mosaics: evidence for a spermatogenesis gene on the mouse Y chromosome. Cytogenet Cell Genet. 1986;42: 208–213. doi:10.1159/000132280

133. Mazeyrat S, Saut N, Grigoriev V, Mahadevaiah SK, Ojarikre OA, Rattigan Á, et al. A Y-encoded subunit of the translation initiation factor Eif2 is essential for mouse spermatogenesis. Nat Genet. 2001;29: 49–53. doi:10.1038/ng717

134. Touré A, Szot M, Mahadevaiah SK, Rattigan A, Ojarikre OA, Burgoyne PS. A new deletion of the mouse Y chromosome long arm associated with the loss of Ssty expression, abnormal sperm development and sterility. Genetics. 2004;166: 901–912.

135. Vernet N, Mahadevaiah SK, Yamauchi Y, Decarpentrie F, Mitchell MJ, Ward MA, et al. Mouse Y-Linked Zfy1 and Zfy2 Are Expressed during the Male-Specific Interphase between Meiosis I and Meiosis II and Promote the 2nd Meiotic Division. PLOS Genetics. 2014;10: e1004444. doi:10.1371/journal.pgen.1004444

136. Yamauchi Y, Riel JM, Stoytcheva Z, Ward MA. Two Y Genes Can Replace the Entire Y Chromosome for Assisted Reproduction in the Mouse. Science. 2014;343: 69–72. doi:10.1126/science.1242544

137. Shaw DE, Ross WD, Lambert AV, White MA. Single cell RNA-sequencing reveals no evidence for meiotic sex chromosome inactivation in the threespine stickleback fish. bioRxiv; 2024. p. 2024.11.26.625488. doi:10.1101/2024.11.26.625488

138. Largiadèr CR, Fries V, Bakker TCM. Genetic analysis of sneaking and egg-thievery in a natural population of the three-spined stickleback (Gasterosteus aculeatus L.). Heredity. 2001;86: 459–468. doi:10.1046/j.1365-2540.2001.00850.x

139. Mehlis M, Rahn AK, Bakker TCM. Sperm quality but not relatedness predicts sperm competition success in threespine sticklebacks (Gasterosteus aculeatus). BMC Evol Biol. 2015;15: 74. doi:10.1186/s12862-015-0353-x

140. Mehlis M, Hilke LK, Bakker TCM. Attractive males have faster sperm in three-spined sticklebacks Gasterosteus aculeatus. Current Zoology. 2013;59: 761–768. doi:10.1093/czoolo/59.6.761

141. Arnold AP, Chen X. What does the “four core genotypes” mouse model tell us about sex differences in the brain and other tissues? Frontiers in Neuroendocrinology. 2009;30: 1–9. doi:10.1016/j.yfrne.2008.11.001

142. Arnold AP. Four Core Genotypes and XY* mouse models: Update on impact on SABV research. Neuroscience & Biobehavioral Reviews. 2020;119: 1–8. doi:10.1016/j.neubiorev.2020.09.021

143. Vries GJD, Rissman EF, Simerly RB, Yang L-Y, Scordalakes EM, Auger CJ, et al. A Model System for Study of Sex Chromosome Effects on Sexually Dimorphic Neural and Behavioral Traits. J Neurosci. 2002;22: 9005–9014. doi:10.1523/JNEUROSCI.22-20-09005.2002

144. Gatewood JD, Wills A, Shetty S, Xu J, Arnold AP, Burgoyne PS, et al. Sex Chromosome Complement and Gonadal Sex Influence Aggressive and Parental Behaviors in Mice. J Neurosci. 2006;26: 2335–2342. doi:10.1523/JNEUROSCI.3743-05.2006

145. Suster ML, Abe G, Schouw A, Kawakami K. Transposon-mediated BAC transgenesis in zebrafish. Nat Protoc. 2011;6: 1998–2021. doi:10.1038/nprot.2011.416

146. Montague TG, Cruz JM, Gagnon JA, Church GM, Valen E. CHOPCHOP: a CRISPR/Cas9 and TALEN web tool for genome editing. Nucleic Acids Research. 2014;42: W401–W407. doi:10.1093/nar/gku410

147. Labun K, Montague TG, Gagnon JA, Thyme SB, Valen E. CHOPCHOP v2: a web tool for the next generation of CRISPR genome engineering. Nucleic Acids Research. 2016;44: W272–W276. doi:10.1093/nar/gkw398

148. Labun K, Montague TG, Krause M, Torres Cleuren YN, Tjeldnes H, Valen E. CHOPCHOP v3: expanding the CRISPR web toolbox beyond genome editing. Nucleic Acids Research. 2019;47: W171–W174. doi:10.1093/nar/gkz365

149. Subedi A, Macurak M, Gee ST, Monge E, Goll MG, Potter CJ, et al. Adoption of the Q transcriptional regulatory system for zebrafish transgenesis. Methods. 2014;66: 433–440. doi:10.1016/j.ymeth.2013.06.012

150. Kingsley DM, Zhu B, Osoegawa K, De Jong PJ, Schein J, Marra M, et al. New Genomic Tools for Molecular Studies of Evolutionary Change in Threespine Sticklebacks. Behaviour. 2004;141: 1331–1344.

151. Archambeault SL, Bärtschi LR, Merminod AD, Peichel CL. Adaptation via pleiotropy and linkage: Association mapping reveals a complex genetic architecture within the stickleback Eda locus. Evolution Letters. 2020;4: 282–301. doi:10.1002/evl3.175

152. Schindelin J, Arganda-Carreras I, Frise E, Kaynig V, Longair M, Pietzsch T, et al. Fiji: an open-source platform for biological-image analysis. Nat Methods. 2012;9: 676–682. doi:10.1038/nmeth.2019

153. Collins III JJ, Hou X, Romanova EV, Lambrus BG, Miller CM, Saberi A, et al. Genome-Wide Analyses Reveal a Role for Peptide Hormones in Planarian Germline Development. PLOS Biology. 2010;8: e1000509. doi:10.1371/journal.pbio.1000509

154. Square TA, Sundaram S, Mackey EJ, Miller CT. Distinct tooth regeneration systems deploy a conserved battery of genes. EvoDevo. 2021;12: 4. doi:10.1186/s13227-021-00172-3

155. Edgar RC. Muscle5: High-accuracy alignment ensembles enable unbiased assessments of sequence homology and phylogeny. Nat Commun. 2022;13: 6968. doi:10.1038/s41467-022-34630-w

156. Paradis E, Schliep K. ape 5.0: an environment for modern phylogenetics and evolutionary analyses in R. Bioinformatics. 2019;35: 526–528. doi:10.1093/bioinformatics/bty633

157. Mayor C, Brudno M, Schwartz JR, Poliakov A, Rubin EM, Frazer KA, et al. VISTA : visualizing global DNA sequence alignments of arbitrary length. Bioinformatics. 2000;16: 1046–1047. doi:10.1093/bioinformatics/16.11.1046

158. Frazer KA, Pachter L, Poliakov A, Rubin EM, Dubchak I. VISTA: computational tools for comparative genomics. Nucleic Acids Research. 2004;32: W273–W279. doi:10.1093/nar/gkh458

159. Brudno M, Do CB, Cooper GM, Kim MF, Davydov E, Program NCS, et al. LAGAN and Multi-LAGAN: Efficient Tools for Large-Scale Multiple Alignment of Genomic DNA. Genome Res. 2003;13: 721–731. doi:10.1101/gr.926603

160. Bolger AM, Lohse M, Usadel B. Trimmomatic: a flexible trimmer for Illumina sequence data. Bioinformatics. 2014;30: 2114–2120. doi:10.1093/bioinformatics/btu170

161. Zhang Y, Park C, Bennett C, Thornton M, Kim D. Rapid and accurate alignment of nucleotide conversion sequencing reads with HISAT-3N. Genome Res. 2021;31: 1290–1295. doi:10.1101/gr.275193.120

162. Putri GH, Anders S, Pyl PT, Pimanda JE, Zanini F. Analysing high-throughput sequencing data in Python with HTSeq 2.0. Bioinformatics. 2022;38: 2943–2945. doi:10.1093/bioinformatics/btac166

163. Love MI, Huber W, Anders S. Moderated estimation of fold change and dispersion for RNA-seq data with DESeq2. Genome Biology. 2014;15: 550. doi:10.1186/s13059-014-0550-8